Rigorous Upscaling of Unsaturated Flow in Fractured Porous Media

DOI: 10.1137/18M1203754
Handle: http://hdl.handle.net/1942/30983

RIGOROUS UPSCALING OF UNSATURATED FLOW IN FRACTURED POROUS MEDIA *

FLORIAN LIST †, ‡, KUNDAN KUMAR §, ¶, IULIU SORIN POP ‡, ¶, AND FLORIN ADRIAN RADU ¶

Abstract. In this work, we consider a mathematical model for flow in an unsaturated porous medium containing a fracture. In all subdomains (the fracture and the adjacent matrix blocks) the flow is governed by Richards' equation. The submodels are coupled by physical transmission conditions expressing the continuity of the normal fluxes and of the pressures. We start by analyzing the case of a fracture having a fixed width-length ratio, called $\varepsilon > 0$. Then we take the limit $\varepsilon \to 0$ and give a rigorous proof for the convergence towards effective models. This is done in different regimes, depending on how the ratio of porosities and permeabilities in the fracture, respectively in the matrix, scale in terms of ε, and leads to a variety of effective models. Numerical simulations confirm the theoretical upscaling results.

Key words. Richards' equation, Fractured porous media, Upscaling, Unsaturated flow in porous media, Existence and uniqueness of weak solutions

AMS subject classifications. 35B27, 35A35, 35J25, 35K65,

1. Introduction.

Fractured porous media arise in a multitude of environmental and technical applications, including fragmented rocks, hydraulic fracturing, carbon dioxide sequestration, and geothermal systems. Fractures are thin formations, in which the hydraulic properties such as porosity and permeability differ significantly from those of the surrounding matrix blocks. Hence, fractures have a crucial impact on fluid flow [1], and fractures or entire fracture networks must be incorporated in the mathematical models for fluid flow. This is challenging from the numerical point of view, firstly due to the high geometrical complexity of fracture networks and secondly because grid cells with a high aspect ratio or a very fine grid resolution within the fractures and in the adjacent matrix region are required.

In order to overcome the latter difficulty, it is appealing to embed fractures as lower-dimensional manifolds into a higher-dimensional domain (e.g. as lines in a two-dimensional domain). Such models are also referred to as mixed-dimensional models, or hybrid-dimensional models, or Discrete Fracture Network Models (DFN). Depending on the context, fractures may block or conduct fluid flow, which can be expressed for example by coupling the mathematical model for the matrix blocks with a differential equation on the lower-dimensional fractures. Herein, we prove that such models result naturally from models with positive fracture width in the limit case where the width passes to zero. The presented model in this work provides a physically-consistent foundation for discrete fracture modeling approaches as used e.g. in [28, 39, 64]).

We consider a two-dimensional model for unsaturated fluid flow in a fractured porous medium. For the ease of presentation, the geometry is given by two rectangular matrix blocks, separated by a single fracture. Here we assume that, next to the matrix blocks, the fracture is a porous medium too, as encountered e.g. in the case of

*Submitted to the editors DATE.

Funding: NFR, NWO, Norwegian Academy of Science, FWO, Statoil

†School of Physics, University of Sydney, Australia, flis0155@uni.sydney.edu.au

‡Department of Mathematics, University of Hasselt, Belgium, {florian.list, sorin.pop}@uhasselt.be

§Department of Mathematics, Karlstad University, Sweden, kundan.kumar@kau.se

¶Department of Mathematics, University of Bergen, Norway, Florin.Radu@uib.no

sediment-filled fractures [35], or layered porous media [53]. We assume that the pore space of the porous medium is filled with a liquid (say, water) and air. Provided that the domain is interconnected and connected to the surface, the assumption that the air is infinitely mobile is justified, and the air pressure can be set to zero in the full two-phase model. In this way, the governing model in the matrix blocks and in the fracture is the Richards equation [60],

$$\partial_t(\Phi S(\psi)) - \nabla \cdot (K_a K(S(\psi))\nabla\psi) = f. \tag{1}$$

Here, ψ denotes the pressure head, Φ the porosity of the medium, S the water saturation, K_a and K stand for the absolute, respective relative hydraulic conductivity, and f is a source or sink term. For simplicity, the gravity is neglected, and the absolute permeability is a scalar, but all the results in this paper can be extended to include gravity, or anisotropic media.

In (1), Φ and K_a are medium-dependent parameters. Similarly, the water saturation S is a given, increasing function of ψ, whereas the relative conductivity K is a given function of S. As for Φ and K_a, these relationships depend on the type of the material in the porous medium. Therefore, all these material properties may be different in the fracture and in the matrix blocks, see e.g. [33]. Well-known are the van Genuchten–Mualem [29] and Brooks–Corey [15] relationships.

The Richards equation is a nonlinear parabolic partial differential equation and may degenerate wherever the flow is saturated $S'(\psi) = 0$ (the fast diffusion case) or $K(S(\psi)) \to 0$ (the slow diffusion case). However, the rigorous mathematical results in this work only cover non-degenerate cases, when the medium is strictly unsaturated. On the other hand, the effective models derived here remain formally valid also in the degenerate cases.

In view of its practical relevance, the Richards equation has been investigated thoroughly in the mathematical literature. Without being exhaustive, we mention [4, 5, 19] for results concerning the existence of weak solutions including degenerate cases. Uniqueness results are obtained in e.g. [55, 56]. The numerical methods are developed in agreement with the analytical results. One remarkable feature is that when compared to the case of the heat equation, the solutions to the Richards equation lack regularity. For this reason, as well as for ensuring stability, the implicit Euler scheme is commonly used for the time discretisation. The outcome is a sequence of time discrete nonlinear elliptic equations, which are generally solved by means of linear iterative schemes like Newton, fixed-point or Picard. Such methods are discussed and compared e.g. in [44, 48]. For the spatial discretisation, we mention [23, 24, 40] where finite volume approaches are presented, [8, 59, 70] for mixed finite element methods, and [22, 54] for finite element schemes.

In all papers mentioned above, the parameters and nonlinearities are either fixed over the entire domain, or vary smoothly. In other words, the problems can be considered over the entire domain, without paying particular attention to the fact that there are different media involved. In the present work, the medium consists of different homogeneous blocks, connected through transmission conditions that will be given below. In this context, domain decomposition methods represent an efficient way to reduce both the problem complexity, and to deal with the occurrence of different homogeneous blocks. We refer to [11] for a domain decomposition scheme applied to unsaturated flows in layered soils, and to [63] for a scheme combining linearisation and domain decomposition techniques in each iteration.

The present work considers a particular situation, where the medium consists of two homogeneous blocks, separated by a thin, homogeneous structure, that is the

fracture. We assume a two-dimensional situation and let $\varepsilon > 0$ be a dimensionless number giving the ratio between the fracture width and length. Since the fracture is assumed thin, ε can be seen as a small parameter. If fractures are viewed as two-dimensional objects, their discretisation becomes complex as the mesh should either contain anisotropic elements respecting the fracture shape, or should be extremely fine. To avoid such issues, one possibility is to approximate fractures as lower dimensional elements in the entire domain. This implies finding appropriate, reduced dimensional models for the fracture, and how these are connected to the models in the matrix blocks. In this sense, we mention [6, 46], where the reduced dimensional models for two-phase flow, respective reactive transport in fractured media are derived by formal arguments based on a transversal averaging of the model inside fractures. Similar results, but using anisotropic asymptotic expansion methods in terms of ε are obtained in [20, 49, 50, 51, 57], where the convergence of the averaging process is proved rigorously when $\varepsilon \searrow 0$. However, the models considered there are either linear, or the nonlinearities appear through reaction terms or the conditions coupling the models in two adjacent homogeneous sub-domains. We also refer to [2, 14, 26, 27], where reduced dimensional models for flow in fractured media are presented with emphasis on developing appropriate numerical schemes.

The models considered here assume that the pressure is continuous at the interfaces separating the matrix blocks and the fracture. In other words, entry pressure models leading to the extended pressure condition derived in [18] are disregarded. For such models we also mention that homogenisation results are obtained in [21, 34, 62, 66]. In particular, oil trapping effects are well explained by such models. Although the pressure is assumed continuous at the interfaces separating the homogeneous blocks, this does not rule out the situation where the averaged pressure across a fracture may still become discontinuous in the reduced dimensional models. Such models are discussed e.g. in [2, 7, 12]. The present analysis does not cover such cases, but we refer to [41, 43] for the formal derivation of such models in the specific context discussed here.

Still referring to fractured media, but with a different motivation, are the works in [47] for a phase field model describing the propagation of fluid filled fractures and [31] for iterative approaches to static fractures.

The main goal in this work is to give a mathematically rigorous derivation of the reduced dimensional models in fractured media. More precise, we give rigorous proofs for the convergence of the transversal averaging procedure when passing ε, the ratio between the fracture width and length, to zero. Depending on how the ratio of the porosities and of the absolute permeabilities in the different types of materials scale w.r.t. ε, five different reduced dimensional models are obtained. More precisely, if the fracture is more permeable than the adjacent blocks, it becomes a preferential flow path. On the contrary, if the fracture is less permeable than the blocks, the fluid will have a preference to flow in the blocks. In consequence, the reduced dimensional fracture equation for the fracture can be an interface condition or a differential equation. Such results are obtained by means of a formal derivation in [3, 46]. Our approach is in spirit of [49, 50, 51, 67], where the single phase flow through a highly permeable fracture is considered. In the cases mentioned above, this corresponds to a particular choice of the scaling in the porosity ratio, respectively the absolute permeability ratio.

In this paper we consider the case of an unsaturated porous media flow, which is modeled through a nonlinear parabolic problem but with different nonlinearities in the matrix, respectively the fracture. We consider different scalings in the permeability

and porosity ratios, and give the rigorous mathematical justification of the averaging process that leads to a reduced dimensional fracture model when $\varepsilon \searrow 0$. In one of the five cases considered here, we obtain a widely used fracture model. To our knowledge, this is the first rigorous mathematical justification given for such models, existing results in this sense being restricted to formal asymptotic arguments. Next to this, other four different classes of models are obtained rigorously, depending on the above mentioned scaling in the permeabilities and the porosities.

The outline of this work is as follows. In Section 2, the coupled model is formulated, and a non-dimensionalisation procedure is carried out in order to derive a dimensionless model, which is then used for the upscaling. Two scaling parameters, κ and λ, are introduced. These account for the scaling of the porosities and absolute hydraulic conductivities with respect to ε. In Section 3, we briefly state the main results of this work. Section 4 is concerned with the existence of solutions to the model for a constant but positive fracture width, i.e. $\varepsilon > 0$. This is done by applying Rothe's method (see e.g. [38]). Based on compactness arguments we prove the existence of solutions to the coupled model. Further, to reduce the dimensionality of the fracture, we investigate the limit of vanishing fracture width, that is $\varepsilon \to 0$ in Section 5. Section 6 presents numerical simulations that confirm our theoretical upscaling results.

2. Model. First, we formulate the model in dimensional form. Thereafter, we introduce reference quantities and make assumptions on their scaling with respect to one another. This is where the scaling parameters κ and λ come into play. By relating the dimensional quantities to the reference quantities, the non-dimensional model is derived, which will be considered in the subsequent sections.

2.1. Dimensional model. We resort to a simple two-dimensional geometry consisting of two square solid matrix blocks with edge length L separated by a fracture of width l. The geometry is illustrated in Figure 1 (left).

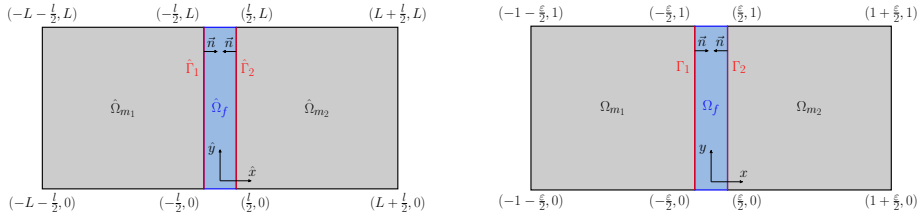

FIG. 1. *Dimensional (left) and dimensionless (right) geometry of the fracture and the surrounding matrix blocks*

The subscripts m and f indicate the matrix blocks and the fracture, respectively. They are defined as

$$\begin{aligned} \hat{\Omega}_{m_1} &:= \left(-L-\frac{l}{2},-\frac{l}{2}\right)\times(0,L), & \hat{\Gamma}_1 &:= \left\{-\frac{l}{2}\right\}\times(0,L),\\ \hat{\Omega}_{m_2} &:= \left(\frac{l}{2},L+\frac{l}{2}\right)\times(0,L), & \hat{\Gamma}_2 &:= \left\{\frac{l}{2}\right\}\times(0,L),\\ \hat{\Omega}_f &:= \left(-\frac{l}{2},\frac{l}{2}\right)\times(0,L). \end{aligned} \tag{2}$$

We use superscript hats for denoting quantities associated with the dimensional model in order to distinguish them from the dimensionless quantities which will be introduced

subsequently.
The model defined on the dimensional geometry is given by

Problem $\mathcal{P}_D$:

$$
\begin{cases}
\partial_{\hat{t}}(\Phi_m \hat{S}_m(\hat{\psi}_{m_j})) + \hat{\nabla}\cdot \hat{v}_{m_j} = \hat{f}_{m_j} & \text{in } \hat{\Omega}_{m_j}^{\hat{T}},\\
\hat{v}_{m_j} = -\hat{K}_{a,m}\hat{K}_m(\hat{S}_m(\hat{\psi}_{m_j}))\hat{\nabla}\hat{\psi}_{m_j} & \text{in } \hat{\Omega}_{m_j}^{\hat{T}},\\
\partial_{\hat{t}}(\Phi_f \hat{S}_f(\hat{\psi}_f)) + \hat{\nabla}\cdot \hat{v}_f = \hat{f}_f & \text{in } \hat{\Omega}_f^{\hat{T}},\\
\hat{v}_f = -\hat{K}_{a,f}\hat{K}_f(\hat{S}_f(\hat{\psi}_f))\hat{\nabla}\hat{\psi}_f & \text{in } \hat{\Omega}_f^{\hat{T}},\\
\hat{v}_{m_j}\cdot\vec{n} = \hat{v}_f\cdot\vec{n} & \text{on } \hat{\Gamma}_j^{\hat{T}},\\
\hat{\psi}_{m_j} = \hat{\psi}_f & \text{on } \hat{\Gamma}_j^{\hat{T}},\\
\hat{\psi}_\rho(0) = \hat{\psi}_{\rho,I} & \text{in } \hat{\Omega}_\rho,
\end{cases}
$$

for $\rho \in \{m_1, m_2, f\}$, $j \in \{1,2\}$, where $\hat{\Omega}_m := \hat{\Omega}_{m_1} \cup \hat{\Omega}_{m_2}$, and where we set $\Omega_\rho^{\hat{T}} := \Omega_\rho \times (0, \hat{T}]$ for all spatial domains Ω_ρ and a given final time $\hat{T} > 0$. Furthermore, $\vec{n}$ is a normal vector pointing from $\hat{\Omega}_{m_j}$ into $\hat{\Omega}_f$. $\hat{S}_\rho$, $\hat{v}_\rho$, $\hat{\psi}_\rho$, $\hat{K}_{a,\rho}$, $\hat{K}_\rho$ are the saturation, flux, pressure height, absolute and relative hydraulic conductivities in the subdomain Ω_ρ, respectively. $\hat{\psi}_{\rho,I}$ is a given initial condition and $\hat{f}_\rho$ is a source/sink term. To complete the model, boundary conditions are needed at the outer boundaries of the medium. For simplicity we assume that the pressure vanishes there.

From an application point of view, the flow in the fracture and in the matrix blocks is modelled by the Richards equation, supplemented with the continuity of the normal fluxes and of the pressures as transmission conditions at the interfaces separating two homogeneous subdomains.

2.2. Non-dimensionalisation. We define $\varepsilon := \frac{l}{L}$, that is, the ratio of the fracture width to its length. We take L as the reference length scale. The dimensionless geometry is as shown in Figure 1 (right):

$$
\begin{aligned}
\Omega_{m_1} &= \left(-1-\frac{\varepsilon}{2}, -\frac{\varepsilon}{2}\right)\times(0,1), & \Gamma_1 &= \left\{-\frac{\varepsilon}{2}\right\}\times(0,1),\\
\Omega_{m_2} &= \left(\frac{\varepsilon}{2}, 1+\frac{\varepsilon}{2}\right)\times(0,1), & \Gamma_2 &= \left\{\frac{\varepsilon}{2}\right\}\times(0,1),\\
\Omega_f &= \left(-\frac{\varepsilon}{2}, \frac{\varepsilon}{2}\right)\times(0,1).
\end{aligned}
\tag{3}
$$

Since the pressure is continuous at the interfaces, we define a single reference pressure head for the entire domain, $\bar{\psi} = L$. We further assume that the matrix blocks have the same properties. Consequently, only two absolute hydraulic conductivities are encountered, $\hat{K}_{a,m}$ and $\hat{K}_{a,f}$, respectively. As reference time scale we set

$$
\bar{T} := \frac{\Phi_m L^2}{\hat{K}_{a,m}\bar{\psi}} = \frac{\Phi_m L}{\hat{K}_{a,m}}. \tag{4}
$$

The dimensionless pressure heads are then given as $\psi_{m_j} = \hat{\psi}_{m_j}/L$ and $\psi_f = \hat{\psi}_f/L$, the dimensionless time as $t = \hat{t}/\bar{T}$, and the final time as $T = \hat{T}/\bar{T}$. As regards the source terms, we set $f_{m_j} = \hat{f}_{m_j}\bar{T}/\Phi_m$ and $f_f = \hat{f}_f\bar{T}/\Phi_m$.

The functions $\hat{S}_\rho$ and $\hat{K}_\rho$ (where $\rho \in \{m_1, m_2, f\}$) are dimensionless. Expressed in terms of dimensionless arguments, they become S_ρ and K_ρ.

Using the Darcy law in the mass balance equation in Problem $\mathcal{P}_D$ and using (4), one gets the dimensionless equations for the matrix blocks ($j \in \{1, 2\}$)

$$\partial_t S_m(\psi_{m_j}) - \nabla \cdot \left(K_m(S_m(\psi_{m_j}))\nabla\psi_{m_j}\right) = f_{m_j} \quad \text{in } \Omega^T_{m_j}. \tag{5}$$

As announced in the introduction, the results depend on the types of materials in the blocks and in the fractures. More exactly, important is how the ratio of the porosities and of the absolute hydraulic conductivities in the fracture and the matrix blocks scale w.r.t. ε,

$$\frac{\Phi_f}{\Phi_m} \propto \varepsilon^\kappa, \quad \text{and} \quad \frac{\hat{K}_{a,f}}{\hat{K}_{a,m}} \propto \varepsilon^\lambda. \tag{6}$$

Here $\kappa, \lambda \in \mathbb{R}$ are scaling parameters. For the ease of notation, we take the constants of proportionality to be one for the analysis. Using this and applying the same ideas as above, the model in the fracture becomes

$$\partial_t(\varepsilon^\kappa S_f(\psi_f)) - \nabla \cdot \left(\varepsilon^\lambda K_f(S_f(\psi_f))\nabla\psi_f\right) = f_f \quad \text{in } \Omega^T_f. \tag{7}$$

The transmission condition for the normal flux transforms into

$$K_m(S_m(\psi_{m_j}))\nabla\psi_{m_j} \cdot \vec{n} = \varepsilon^\lambda K_f(S_f(\psi_f))\nabla\psi_f \cdot \vec{n} \qquad \text{on } \Gamma^T_j. \tag{8}$$

In what follows, the dimensionless fracture width $\varepsilon > 0$ is a model parameter. Given $\varepsilon > 0$, the dimensionless model becomes

$$\text{Problem } \mathcal{P}_\varepsilon : \begin{cases} \partial_t S_m(\psi^\varepsilon_{m_j}) + \nabla \cdot v^\varepsilon_{m_j} = f_{m_j} & \text{in } \Omega^T_{m_j}, \\ v^\varepsilon_{m_j} = -K_m(S_m(\psi^\varepsilon_{m_j}))\nabla\psi^\varepsilon_{m_j} & \text{in } \Omega^T_{m_j}, \\ \partial_t(\varepsilon^\kappa S_f(\psi^\varepsilon_f)) + \nabla \cdot v^\varepsilon_f = f^\varepsilon_f & \text{in } \Omega^T_f, \\ v^\varepsilon_f = -\varepsilon^\lambda K_f(S_f(\psi^\varepsilon_f))\nabla\psi^\varepsilon_f & \text{in } \Omega^T_f, \\ v^\varepsilon_{m_j} \cdot \vec{n} = v^\varepsilon_f \cdot \vec{n} & \text{on } \Gamma^T_j, \\ \psi^\varepsilon_{m_j} = \psi^\varepsilon_f & \text{on } \Gamma^T_j, \\ \psi^\varepsilon_\rho(0) = \psi_{\rho,I} & \text{in } \Omega_\rho. \end{cases} \tag{$\mathcal{P}_\varepsilon$}$$

As mentioned before, homogeneous boundary conditions are imposed at the outer boundary.

Remark 1 (Scaling parameters). The scaling parameters $\kappa, \lambda \in \mathbb{R}$ will be crucial in determining the effective models in the limit $\varepsilon \to 0$. κ is related to the storage capacity of the fracture: for $\kappa < 0$, the reference porosity of the fracture increases for decreasing ε as compared to the reference porosity of the matrix blocks. Moreover, if $\kappa \leq -1$, a storage term will be present in the reduced dimensional fracture model, meaning that the fracture maintains its ability to store water as ε approaches zero. For $\kappa = 0$, no scaling occurs, and for $\kappa > 0$, the storage ability of the fracture decreases for $\varepsilon \to 0$ due to the decline of both the fracture volume (assuming fixed L) and of the fracture porosity.

The parameter λ instead gives the scaling of the conductivities. Here we consider the case $\lambda < 1$. $\lambda < 0$ corresponds to the case of a highly conductive fracture when compared to the matrix, which means that the flow through the fracture is more rapid. Whenever $\lambda > 0$ the fracture is less permeable than the blocks. The case

$\lambda = 0$ means comparable conductivities. The case $\lambda \geq 1$ corresponds to impermeable fractures, leading in the limit $\varepsilon \to 0$ to models where the pressures at the matrix block at each side of the fractures are discontinuous (see [43]). To analyze such cases rigorously, one can employ techniques that are similar to ones used in [52], which are different from those used here. Accordingly, we only restrict to the case when $\lambda < 1$.

3. Main result. Our main result is the rigorous derivation of effective models replacing the fracture by an interface. Table 1 provides a brief summary of the effective models for the entire range $(\kappa, \lambda) \in [-1, \infty) \times (-\infty, 1)$ except for the case when $\kappa = -1, \lambda \in (-1, 1)$. Due to the nonlinearity of the time derivative term involved, the identification of the limit requires stronger estimates than we have. Therefore, this case is left out in this paper, but we refer to [41, 43] for the formal derivation.

	Fracture equation	Parameter range for (κ, λ)
Effective model I	Richards' equation	$\{-1\} \times \{-1\}$
Effective model II	Elliptic equation	$(-1, \infty) \times \{-1\}$
Effective model III	ODE for spatially constant pressure	$\{-1\} \times (-\infty, -1)$
Effective model IV	Spatially constant pressure	$(-1, \infty) \times (-\infty, -1)$
Effective model V	Pressure and flux continuity between matrix blocks	$(-1, \infty) \times (-1, 1)$

TABLE 1
Summary of the effective models

We state the strong formulation of the effective models, obtained for $(\kappa, \lambda) \in [-1, \infty) \times (-\infty, 1)$ excepting the case $\kappa = -1, \lambda \in (-1, 1)$. To this aim, we introduce the reduced dimensional fracture domain $\Gamma = \{0\} \times (0, 1)$ and let $\Gamma^T = \Gamma \times (0, T]$.

3.1. Effective models: strong formulation. Effective model I consists of Richards' equation in the matrix block subdomains and the one-dimensional Richards equation in the fracture. It occurs for $\kappa = \lambda = -1$.

Effective model I:

$$
\begin{cases}
\partial_t S_m(\psi_{m_j}) - \nabla \cdot \left(K_m(S_m(\psi_{m_j}))\nabla\psi_{m_j}\right) = f_{m_j}, & \text{in } \Omega_{m_j}^T, \\
\partial_t S_f(\psi_f) - \partial_y \left(K_f(S_f(\psi_f))\partial_y\psi_f\right) = [\vec{q}_m]_\Gamma, & \text{on } \Gamma^T, \\
\psi_{m_j} = \psi_f, & \text{on } \Gamma^T, \\
\psi_{m_j}(0) = \psi_{m_j,I}, & \text{on } \Omega_{m_j}, \\
\psi_f(0) = \psi_{f,I}, & \text{on } \Gamma,
\end{cases}
\tag{9}
$$

where

$$
[\vec{q}_m]_\Gamma := \left(K_m(S_m(\psi_{m_1}))\nabla\psi_{m_1} \cdot \vec{n}_{m_1} + K_m(S_m(\psi_{m_2}))\nabla\psi_{m_2} \cdot \vec{n}_{m_2}\right)\big|_\Gamma \tag{10}
$$

is the flux difference between the two solid matrix subdomains acting as a source term for Richards' equation in the fracture (note that $\vec{n}_{m_1} = -\vec{n}_{m_2}$). Since this is the commonly used model when considering reduced-dimensional fracture models, we emphasise that it can be derived rigorously only for the scaling $\kappa = \lambda = -1$.

If the porosity ratio changes slower w.r.t. the fracture aspect ratio than assumed before, whereas the permeability ratio remains proportional to the reciprocal of this aspect ratio, i.e. $\kappa > -1$ and $\lambda = -1$, then the time derivative term vanishes in the fracture model and one ends up with an effective model consisting of the Richards equation in the matrix blocks and an elliptic equation in the fracture.

Effective model II:

$$\begin{cases} \partial_t S_m(\psi_{m_j}) - \nabla \cdot \left(K_m(S_m(\psi_{m_j}))\nabla\psi_{m_j}\right) = f_{m_j}, & \text{in } \Omega_{m_j}^T, \\ -\partial_y \left(K_f(S_f(\psi_f))\partial_y\psi_f\right) = [\vec{q}_m]_\Gamma, & \text{on } \Gamma^T, \\ \psi_{m_j} = \psi_f, & \text{on } \Gamma^T, \\ \psi_{m_j}(0) = \psi_{m_j,I}, & \text{on } \Omega_{m_j}. \end{cases} \tag{11}$$

For $\kappa = -1$ and $\lambda < -1$, the pressure in the fracture becomes constant in space in the effective model, and due to the pressure continuity, it acts as the boundary condition for the pressure in the matrices. This happens because the permeability in the fracture becomes so large compared to the one in the blocks that in the limit $\varepsilon \searrow 0$, pressure differences in the fracture are instantaneously equilibrated.

Effective model III:

$$\begin{cases} \partial_t S_m(\psi_{m_j}) - \nabla \cdot \left(K_m(S_m(\psi_{m_j}))\nabla\psi_{m_j}\right) = f_{m_j}, & \text{in } \Omega_{m_j}^T, \\ \psi_f(t,y) = \psi_f(t), & \text{on } \Gamma^T, \\ \partial_t S_f(\psi_f)(t) = \displaystyle\int_0^1 [\vec{q}_m]_\Gamma \ dy, & \text{on } \Gamma^T, \\ \psi_{m_j} = \psi_f, & \text{on } \Gamma^T, \\ \psi_{m_j}(0) = \psi_{m_j,I}, & \text{on } \Omega_{m_j}, \\ \psi_f(0) = \psi_{f,I}, & \text{on } \Gamma. \end{cases} \tag{12}$$

For $\kappa > -1$ and $\lambda < -1$, the pressure in the fracture takes a constant value at each time, in such a way that the total flux across the fracture is conserved. This is actually a combination of the last two cases above, since both the time derivative and the capillary effects disappear in the effective fracture model. The fracture pressure is constant in space, and determined in such a way that the total flux across the fracture is continuous:

Effective model IV:

$$\begin{cases} \partial_t S_m(\psi_{m_j}) - \nabla \cdot \left(K_m(S_m(\psi_{m_j}))\nabla\psi_{m_j}\right) = f_{m_j}, & \text{in } \Omega_{m_j}^T, \\ \psi_f(t,y) = \psi_f(t), & \text{on } \Gamma^T, \\ \displaystyle\int_0^1 [\vec{q}_m]_\Gamma \ dy = 0, & \text{on } \Gamma^T, \\ \psi_{m_j} = \psi_f, & \text{on } \Gamma^T, \\ \psi_{m_j}(0) = \psi_{m_j,I}, & \text{on } \Omega_{m_j}. \end{cases} \tag{13}$$

For $\kappa > -1$ and $\lambda \in (-1, 1)$, an effective model results in which the fracture as a physical entity has disappeared. One can therefore disregard the fracture in the effective model. In this case, both the pressure and the flux are continuous on Γ.

Effective model V:

$$\begin{cases} \partial_t S_m(\psi_{m_j}) - \nabla \cdot \left(K_m(S_m(\psi_{m_j}))\nabla\psi_{m_j}\right) = f_{m_j}, & \text{in } \Omega_{m_j}^T, \\ [\vec{q}_m]_\Gamma = 0, & \text{on } \Gamma^T, \\ \psi_{m_j} = \psi_f, & \text{on } \Gamma^T, \\ \psi_{m_j}(0) = \psi_{m_j,I}, & \text{on } \Omega_{m_j}. \end{cases} \tag{14}$$

Remark 2 (Spatially constant pressure). For Effective models III and IV, the large permeability in the fracture leads to a constant pressure along the fracture domain. This can naturally occur only in case the pressure is not fixed at different values at the fracture boundaries. For homogeneous Dirichlet conditions, the pressures are prescribed at the boundaries but have an identical value such that the zero function is the only allowed solution in the fracture. However, our results generalise to the case of homogeneous Neumann boundary conditions in the fracture where the spatially constant pressure in the fracture may vary over time.

In practice, the prescription of a suitable effective model can be done as follows: assuming that both the geometric and the hydraulic properties including porosity and permeability are given for several fractures and a porous matrix, the geometric description allows to identify ε (the characteristic width-to-length ratio). One then estimates the scaling of permeability and porosity as a power of ε. This gives λ and κ, based on which the catalogue of models provides the appropriate upscaled model.

3.2. Comparison with existing models. We make a brief comparison with the fracture models that are widely used in practice (see e.g., [32, 61]). We refer to [46] where similar models are derived for single phase flow, but the interface conditions are relevant to us (see for example [3] for the extension to two-phase flow models).

In contrast to the formal derivation in [46] our approach is mathematically rigorous once we assume a scaling of hydraulic properties on ε. Moreover in the models proposed therein, the closure condition introduces a parameter in the effective model for the fracture. Here, we have a catalogue of models and no additional parameter is necessary.

The interface conditions as derived in [46] for a single phase linear Darcy flow model (Eqns. (3.18), (3.19) on pp. 1672) read

$$\begin{aligned} -\xi v_{m_1}\cdot n_1|_{\Gamma_1} + \alpha_f \psi_{m_1}|_{\Gamma_1} &= -(1-\xi) v_{m_2}\cdot n_2|_{\Gamma_2} + \alpha_f \psi_f, \\ -\xi v_{m_2}\cdot n_2|_{\Gamma_1} + \alpha_f \psi_{m_2}|_{\Gamma_2} &= -(1-\xi) v_{m_1}\cdot n_1|_{\Gamma_1} + \alpha_f \psi_f, \end{aligned}$$

where we once again emphasise that the above results are derived for a single phase steady state flow model. Here, $\alpha_f := \bar{K}_{a,f}/\varepsilon = \varepsilon^{\lambda-1}\bar{K}_{a,m}$ and ξ is a parameter introduced when defining closure conditions. In terms of ε and rearranging terms we have (modulo a constant factor),

$$\begin{aligned} \varepsilon^{\lambda-1}\left(\psi_{m_1}|_{\Gamma_1} - \psi_f\right) &= -(1-\xi) v_{m_2}\cdot n_2|_{\Gamma_2} + \xi v_{m_1}\cdot n_1|_{\Gamma_1}, \\ \varepsilon^{\lambda-1}\left(\psi_{m_2}|_{\Gamma_2} - \psi_f\right) &= -(1-\xi) v_{m_1}\cdot n_1|_{\Gamma_1} + \xi v_{m_2}\cdot n_2|_{\Gamma_2}. \end{aligned}$$

For any value of ξ, for $\lambda < 1$, as ε goes to zero, we get $\psi_1 = \psi_f$ on Γ_1 and $\psi_2 = \psi_f$ on Γ_2 and Γ_1, Γ_2 collapse on the same surface (compare with Effective models I–V). For more detailed comparison for other values of ξ we refer to [41].

4. Existence. This section is concerned with the existence of a (weak) solution to Problem $\mathcal{P}_\varepsilon$ for a fixed fracture width $\varepsilon > 0$. An existence result for a similar, equidimensional model related to two-phase porous media flows has been proven in [25]. Strictly speaking about existence, this result is relevant for this section, and adapting it to the situation considered here (the unsaturated, one-phase flow) would be relatively straightforward. However, the upscaling results in the next sections rely on the a priori estimates, in which the exact scaling in terms of ε needs to be specified explicitly. Therefore instead of adapting the results in [25] to the present case, we

give the proof of the a priori estimates and, as a direct outcome, obtain the existence of a weak solution. We proceed in the spirit of [57], where a linear model for reactive flow with nonlinear transmission conditions at the interfaces is considered. For the sake of readability, we drop the superscript ε since it is fixed throughout this section.

4.1. Notation. In this work, we use common notation from functional analysis. The space $L^2(\Omega)$ contains all real valued square integrable functions on a domain $\Omega \subset \mathbb{R}^d$, and $W^{1,2}(\Omega) \subset L^2(\Omega)$ stands for the subset of functions whose weak first order derivatives lie in $L^2(\Omega)$ as well. Furthermore, Bochner spaces $L^2(0,T;X)$ will be used, where X stands for a Banach space. For all domains $\Omega \subset \mathbb{R}^d$ and time intervals $[0,T]$, we introduce the following abbreviations for the norm and the inner product:

$$\begin{aligned} &\|\cdot\|_{\Omega} := \|\cdot\|_{L^2(\Omega)}, \qquad \text{and} \qquad \|\cdot\|_{\Omega^T} := \|\cdot\|_{L^2(0,T;L^2(\Omega))}, \\ &(\cdot,\cdot)_{\Omega} := (\cdot,\cdot)_{L^2(\Omega)}, \qquad \text{and} \qquad (\cdot,\cdot)_{\Omega^T} := (\cdot,\cdot)_{L^2(0,T;L^2(\Omega))}. \end{aligned} \tag{15}$$

In view of the particular Problem $\mathcal{P}_\varepsilon$, we use the following conventions:

- ρ is the index for the subdomain and takes values in $\{m_1, m_2, f\}$,
- j is the index for specifying the matrix block subdomain and takes values in $\{1,2\}$,
- for functions g which are the same in both matrix block subdomains (such as S, K, ...), we define $g_{m_1} = g_{m_2} =: g_m$, which allows to write e.g. $S_\rho(\psi_\rho)$.

Moreover, $C \geq 0$ is a generic constant.

4.2. Assumptions. For the analysis, we assume that the following conditions are satisfied (here $\rho \in \{m_1, m_2, f\}$):

- (A_f) $f_\rho \in C(0,T;L^2(\Omega_\rho))$ and there exists $M_f > 0$ such that $|f_\rho| \leq M_f$ a.e. in Ω_ρ^T.
- (A_{D_S}) $S_\rho \in C^1(\mathbb{R})$.
- (A_S) There exist $m_S, M_S > 0$ such that $0 < m_S \leq S_\rho'(\psi_\rho) \leq M_S$ for all $\psi_\rho \in \mathbb{R}$.
- (A_{D_K}) $K_\rho \in C^1(\mathbb{R})$ and $K_\rho'(S_\rho) > 0$ for all $S_\rho \in \mathbb{R}$.
- (A_K) There exist $m_K, M_K > 0$ such that $0 < m_K \leq K_\rho(S_\rho) \leq M_K$ for all $S_\rho \in \mathbb{R}$.
- (A_ρ) There exists $M_\rho > 0$ such that $|\psi_{\rho,I}| \leq M_\rho$ a.e. in Ω_ρ.

Moreover, for the rigorous upscaling, we require the following bounds for the initial data and the source term in the fracture:

- $\varepsilon^\lambda \|\psi_{f,I}\|_{\Omega_f}^2 \leq C$,
- $\varepsilon^{-\kappa} \|f_f\|_{\Omega_f^T}^2 \to 0 \quad \text{as} \quad \varepsilon \to 0.$

For the ease of writing, let us suppress the dependency of $\psi_{\rho,I}$ and f_ρ on ε in the notation.

Remark 3 (Assumptions). Note that due to Assumption (A_S), we only consider the regular parabolic case here. Assumption (A_K) excludes the slow diffusion case and guarantees the existence of a minimum positive permeability everywhere. Moreover, for the sake of presentation, we make the assumption $S_\rho(0) = 0$, which can easily be achieved by redefining $S_\rho(\psi) = \tilde{S}_\rho(\psi) - \tilde{S}_\rho(0)$. Assumption (A_S) immediately yields the estimate $\|S_\rho(\psi_\rho)\|_{\Omega_\rho} \leq M_S \|\psi_\rho\|_{\Omega_\rho}$.

4.3. Weak solution. We establish a suitable notion of a solution to Problem $\mathcal{P}_\varepsilon$. For this purpose, we define the function spaces

$$\mathcal{V}_{m_j} \subset W^{1,2}(\Omega_{m_j}), \quad \mathcal{V}_f \subset W^{1,2}(\Omega_f), \tag{16}$$

where the desired boundary conditions are implicitly imposed by the choice of the subspaces $\mathcal{V}_{m_j}$ and $\mathcal{V}_f$. We choose homogeneous Dirichlet conditions for the external boundaries in this section, that is, $\mathcal{V}_{m_j} = \{u \in W^{1,2}(\Omega_{m_j}), u = 0 \text{ on } \partial\Omega_{m_j} \setminus \Gamma_j\}$ (the boundary value should be understood in the sense of traces). This choice of boundary condition simplifies the presentation and extensions to other boundary conditions such as no flow Neumann conditions can be made without major difficulties. Note that these spaces depend on the fixed fracture width ε.

The weak formulation of Problem $\mathcal{P}_\varepsilon$ reads as follows:

DEFINITION 4 (Weak solution). *A triple $(\psi_{m_1}, \psi_{m_2}, \psi_f)$ in the product space $L^2(0,T;\mathcal{V}_{m_1}) \times L^2(0,T;\mathcal{V}_{m_2}) \times L^2(0,T;\mathcal{V}_f)$ is called a weak solution to Problem $\mathcal{P}_\varepsilon$ if*

$$\psi_{m_1} = \psi_f \quad \text{on } \Gamma_1 \quad \text{and} \quad \psi_{m_2} = \psi_f \quad \text{on } \Gamma_2 \quad \text{for a.e. } t \in [0,T], \tag{17}$$

in the sense of traces, and

$$\begin{aligned}
&-\sum_{j=1}^{2} \left(S_m(\psi_{m_j}), \partial_t \phi_{m_j}\right)_{\Omega^T_{m_j}} - \varepsilon^\kappa \left(S_f(\psi_f), \partial_t \phi_f\right)_{\Omega^T_f} \\
&+\sum_{j=1}^{2} \left(K_m(S_m(\psi_{m_j}))\nabla\psi_{m_j}, \nabla\phi_{m_j}\right)_{\Omega^T_{m_j}} + \varepsilon^\lambda \left(K_f(S_f(\psi_f))\nabla\psi_f, \nabla\phi_f\right)_{\Omega^T_f} \\
&= \sum_{j=1}^{2} \left(f_{m_j}, \phi_{m_j}\right)_{\Omega^T_{m_j}} + \left(f_f, \phi_f\right)_{\Omega^T_f} \\
&+\sum_{j=1}^{2} \left(S_m(\psi_{m_j,I}), \phi_{m_j}(0)\right)_{\Omega_{m_j}} + \varepsilon^\kappa \left(S_f(\psi_{f,I}), \phi_f(0)\right)_{\Omega_f},
\end{aligned} \tag{18}$$

for all $(\phi_{m_1}, \phi_{m_2}, \phi_f) \in W^{1,2}(0,T;\mathcal{V}_{m_1}) \times W^{1,2}(0,T;\mathcal{V}_{m_2}) \times W^{1,2}(0,T;\mathcal{V}_f)$ satisfying

$$\phi_{m_1} = \phi_f \quad \text{on } \Gamma_1 \quad \text{and} \quad \phi_{m_2} = \phi_f \quad \text{on } \Gamma_2 \quad \text{for a.e. } t \in [0,T], \tag{19}$$

and

$$\phi_\rho(T) = 0, \qquad \text{for } \rho \in \{m_1, m_2, f\}. \tag{20}$$

Note that it makes sense to evaluate the test functions ϕ_ρ at the times $t = 0$ and $t = T$ in the above definition since the space $W^{1,2}(0,T;\mathcal{V}_\rho)$ is embedded in $C(0,T;\mathcal{V}_\rho)$.

4.4. Time discretisation. In what follows, we discretise the problem in time using an implicit Euler approach, which gives elliptic equations at every discrete time $t_k = k\Delta t$, for $k \in \{0, \dots, N\}$, where $N \in \mathbb{N}$. We assume without loss of generality that $N\Delta t = T$. Here, $\Delta t > 0$ denotes the fixed time step size. Choose $\psi^0_\rho = \psi_{\rho,I}$ and let the sequence of solutions in domain Ω_ρ of the time-discrete problems be given as $\{\psi^k_\rho\}$. Moreover, let $f^k_\rho := f_\rho(t_k)$. The definition of a weak solution to the time-discrete problem is given by

DEFINITION 5. *Let $k > 0$ and let $(\psi^{k-1}_{m_1}, \psi^{k-1}_{m_2}, \psi^{k-1}_f) \in \mathcal{V}_{m_1} \times \mathcal{V}_{m_1} \times \mathcal{V}_f$ be given. We call $(\psi^k_{m_1}, \psi^k_{m_2}, \psi^k_f) \in \mathcal{V}_{m_1} \times \mathcal{V}_{m_1} \times \mathcal{V}_f$ a weak solution to the time-discrete problem at time t_k if it satisfies*

$$\psi^k_{m_1} = \psi^k_f \quad \text{on } \Gamma_1 \quad \text{and} \quad \psi^k_{m_2} = \psi^k_f \quad \text{on } \Gamma_2 \tag{21}$$

in the sense of traces, and

(22)

$$\begin{aligned}
&\sum_{j=1}^{2}\left(S_m(\psi_{m_j}^k),\phi_{m_j}\right)_{\Omega_{m_j}}+\varepsilon^{\kappa}\left(S_f(\psi_f^k),\phi_f\right)_{\Omega_f}\\
&+\Delta t\sum_{j=1}^{2}\left(K_m(S_m(\psi_{m_j}^k))\nabla\psi_{m_j}^k,\nabla\phi_{m_j}\right)_{\Omega_{m_j}}+\varepsilon^{\lambda}\Delta t\left(K_f(S_f(\psi_f^k))\nabla\psi_f^k,\nabla\phi_f\right)_{\Omega_f}\\
=&\Delta t\sum_{j=1}^{2}\left(f_{m_j}^k,\phi_{m_j}\right)_{\Omega_{m_j}}+\Delta t\left(f_f^k,\phi_f\right)_{\Omega_f}\\
&+\sum_{j=1}^{2}\left(S_m(\psi_{m_j}^{k-1}),\phi_{m_j}\right)_{\Omega_{m_j}}+\varepsilon^{\kappa}\left(S_f(\psi_f^{k-1}),\phi_f\right)_{\Omega_f},
\end{aligned}$$

for all $(\phi_{m_1},\phi_{m_2},\phi_f)\in\mathcal{V}_{m_1}\times\mathcal{V}_{m_2}\times\mathcal{V}_f$ *satisfying* $\phi_{m_j}=\phi_f$ *on* Γ_j *for* $j\in\{1,2\}$.

4.5. Existence of solution for the time-discrete problem. We begin with the existence of solution for the time-discrete problem as given in Definition 5. We show that the solution triple $(\psi_{m_1}^k,\psi_{m_2}^k,\psi_f^k)\in\mathcal{V}_{m_1}\times\mathcal{V}_{m_2}\times\mathcal{V}_f$ satisfying Definition 5 can be interpreted as a solution to an elliptic problem having coefficients with possibly jump discontinuities. The existence of solution is thus tantamount to showing that of an elliptic problem defined in the whole domain having possibly discontinuous coefficients. The latter follows from standard elliptic theory. We start by introducing the space $\mathcal{V}$

$$\mathcal{V}:=\{(\psi_{m_1},\psi_{m_2},\psi_f)\in\mathcal{V}_{m_1}\times\mathcal{V}_{m_2}\times\mathcal{V}_f,\ \text{s.t. }\psi_{m_1}=\psi_f\text{ at }\Gamma_1,\ \psi_{m_2}=\psi_f\text{ at }\Gamma_2\},$$

equipped with the norm

$$\|\psi\|_{\mathcal{V}}:=\sqrt{\left(\|\psi_{m_1}\|^2_{W^{1,2}(\Omega_{m_1})}+\|\psi_{m_2}\|^2_{W^{1,2}(\Omega_{m_2})}+\|\psi_f\|^2_{W^{1,2}(\Omega_f)}\right)}.$$

As before, the equalities on the interfaces Γ_1,Γ_2 are in the sense of traces. Below we will use the characteristic function χ_ρ of $\Omega_\rho,\rho\in\{m_1,m_2,f\}$ in defining a function over Ω given a triple in $\mathcal{V}$. In this respect we extend ψ_ρ ($\rho\in\{m_1,m_2,f\}$), now defined on Ω_ρ, to the entire Ω. The specific extension is not relevant since only its restriction to Ω_ρ will be needed. We have the following proposition showing that $\mathcal{V}$ is isomorphic to $W^{1,2}(\Omega)$.

PROPOSITION 6. *Given* $\psi\in W^{1,2}(\Omega)$*, its restriction to* Ω_ρ*,* $\rho\in\{m_1,m_2,f\}$*, defines a triple* $(\psi_{m_1},\psi_{m_2},\psi_f)\in\mathcal{V}$*. Conversely, given* $(\psi_{m_1},\psi_{m_2},\psi_f)\in\mathcal{V}$*,* $\psi=\sum_\rho\psi_\rho\chi_\rho,\rho\in\{m_1,m_2,f\}$ *lies in* $W^{1,2}(\Omega)$.

Proof. We start with the first part. For smooth functions, the assertion is obvious. Using a density argument and trace inequalities on Γ_1 and Γ_2, the extension to $W^{1,2}$ functions is straightforward. For the converse, the boundedness of the L^2 norm is clear. Further, it is sufficient to prove that the weak derivatives of the triple $(\psi_{m_1},\psi_{m_2},\psi_f)\in\mathcal{V}$ are equal to those of ψ restricted to Ω_ρ. For a given triple $(\psi_{m_1},\psi_{m_2},\psi_f)\in\mathcal{V}$, let $\psi=\sum_\rho\psi_\rho\chi_\rho,\rho\in\{m_1,m_2,f\}$. Let ϕ be weak derivative of ψ in the $i-$th direction. Using partial integration, for any smooth function w with compact support in Ω,

$$\int_\Omega\phi w\,dx=-\int_\Omega\psi\partial_i w\,dx=-\sum_\rho\int_{\Omega_\rho}\psi_\rho\partial_i w\,dx.$$

Using partial integration on each subdomain

$$-\sum_\rho \int_{\Omega_\rho} \psi_\rho \partial_i w \, dx = \sum_\rho \int_{\Omega_\rho} \partial_i \psi_\rho w \, dx,$$

where the terms on the boundaries Γ_1, Γ_2 get cancelled due to traces being equal. The last equality shows that ϕ restricted to $\Omega_\rho, \rho \in \{m_1, m_2, f\}$ is equal to the weak derivative of ψ in the i-th direction. This proves the proposition. ∎

Remark 7. With respect to the norm $\|\psi\|_{W^{1,2}(\Omega)} = \sqrt{\|\psi\|^2_\Omega + \|\nabla\psi\|^2_\Omega}$, and the same for the $W^{1,2}$ norm on $\Omega_\rho, \rho \in \{m_1, m_2, f\}$, the isomorphism of $\mathcal{V}$ to $W^{1,2}(\Omega)$ is an isometry.

Next, we consider an elliptic problem defined in the entire domain Ω. For a given triple $(\psi^{k-1}_{m_1}, \psi^{k-1}_{m_2}, \psi^{k-1}_f) \in \mathcal{V}$, define $\psi^{k-1} = \sum_\rho \psi^{k-1}_\rho \chi_\rho, \rho \in \{m_1, m_2, f\}$, and the ψ-dependent functions

$$K = K_{m_1}\chi_{m_1} + \varepsilon^\lambda K_f \chi_f + K_{m_2}\chi_{m_2} \text{ and } S = S_{m_1}\chi_{m_1} + \varepsilon^\kappa S_f \chi_f + S_{m_2}\chi_{m_2}. \tag{23}$$

With this, a solution for Problem P_Ω is defined in

DEFINITION 8 (Weak solution of Problem $\mathcal{P}_\Omega$). *Given ψ^{k-1}, $\psi^k \in W^{1,2}_0(\Omega)$ is a weak solution if for all $\phi \in W^{1,2}_0(\Omega)$ it holds that*

$$\left(S(\psi^k), \phi\right)_\Omega + \Delta t \left(K(S(\psi^k))\nabla\psi^k, \nabla\phi\right)_\Omega = \Delta t \left(f^k, \phi\right)_\Omega + \left(S(\psi^{k-1}), \phi\right)_\Omega. \tag{24}$$

The above problem therefore is a nonlinear elliptic problem with positive elliptic coefficient and a lower order reaction term that is monotone with respect to the unknown, and is piecewise smooth w.r.t. x. The existence of solution in the Hilbert space $W^{1,2}_0(\Omega)$ is proved e.g. in [10, 13]. This is stated in the next lemma.

LEMMA 9. *There exists a weak solution of problem P_Ω in the sense of Definition 8.*

The summary of the above discussion results in the existence of a solution for time discrete problem as per Definition 5 and is given below.

LEMMA 10. *Given $(\psi^{k-1}_{m_1}, \psi^{k-1}_{m_2}, \psi^{k-1}_f) \in \mathcal{V}_{m_1} \times \mathcal{V}_{m_1} \times \mathcal{V}_f$, $k > 0$, there exists a solution triple $(\psi^k_{m_1}, \psi^k_{m_2}, \psi^k_f) \in \mathcal{V}_{m_1} \times \mathcal{V}_{m_1} \times \mathcal{V}_f$ and*

$$\psi^k_{m_1} = \psi^k_f \quad \text{on } \Gamma_1 \quad \text{and} \quad \psi^k_{m_2} = \psi^k_f \quad \text{on } \Gamma_2. \tag{25}$$

Proof. The existence result in Lemma 9 provides $\psi^k \in W^{1,2}_0(\Omega)$. Proposition 6 gives a triple $(\psi^k_{m_1}, \psi^k_{m_2}, \psi^k_f) \in \mathcal{V}_{m_1} \times \mathcal{V}_{m_1} \times \mathcal{V}_f$ satisfying $\psi^k_{m_1} = \psi^k_f$ on Γ_1 and $\psi^k_{m_2} = \psi^k_f$ on Γ_2. Moreover, Proposition 6 states the equality of weak derivatives of ψ^k restricted to Ω_ρ with those of ψ^k_ρ. Starting from (24), this yields the existence result in Lemma 10. ∎

Note that the interface conditions on Γ_1, Γ_2 are those commonly used in applications, the continuity of the normal flux and of the pressures. More involved ones, like nonlinear transmission conditions for the pressure, can appear for porous media flow models involving an entry pressure. In this sense we refer to [17, 18, 21, 36, 37, 53, 57, 62, 66].

4.6. *A priori* **estimates.** We define in each domain the energy functional

$$\mathcal{W}_\rho(\psi_\rho) = \int_0^{\psi_\rho} S'_\rho(\varphi)\,\varphi\; d\varphi, \tag{26}$$

which we will use in the proof of the *a priori* estimates. First, we gather some properties of $\mathcal{W}_\rho$ in a simple lemma, which is based on Assumption (A_S):

LEMMA 11. *The functional $\mathcal{W}_\rho$ satisfies the following inequalities:*

$$\begin{aligned} \mathcal{W}_\rho(\psi_\rho) &\geq 0, \\ \mathcal{W}_\rho(\psi_\rho) - \mathcal{W}_\rho(\xi_\rho) &\leq \psi_\rho(S_\rho(\psi_\rho) - S_\rho(\xi_\rho)), \\ m_S\frac{\psi_\rho^2}{2} \leq \mathcal{W}_\rho(\psi_\rho) &\leq M_S\frac{\psi_\rho^2}{2}, \end{aligned} \tag{27}$$

for all $\psi_\rho, \xi_\rho \in \mathbb{R}$.

We obtain the following estimate for the time-discrete solution:

LEMMA 12 (A priori estimate I). *The solution $(\psi_{m_1}^k, \psi_{m_2}^k, \psi_f^k)$ to the time-discrete problem in Definition 5 satisfies*

$$\begin{aligned} &\sum_{j=1}^{2}\left(\max_{l\in\{1,\dots,N\}}\int_{\Omega_{m_j}} \mathcal{W}_m(\psi_{m_j}^l)\; d\vec{x}\right) + \varepsilon^\kappa \max_{l\in\{1,\dots,N\}}\int_{\Omega_f} \mathcal{W}_f(\psi_f^l)\; d\vec{x} \\ &\quad + \frac{\Delta t\; m_K}{2}\sum_{j=1}^{2}\sum_{k=1}^{N}\|\nabla\psi_{m_j}^k\|_{\Omega_{m_j}}^2 + \varepsilon^\lambda\frac{\Delta t\; m_K}{2}\sum_{k=1}^{N}\|\nabla\psi_f^k\|_{\Omega_f}^2 \\ &\leq \sum_{j=1}^{2}\int_{\Omega_{m_j}} \mathcal{W}_m(\psi_{m_j,I})\; d\vec{x} + \varepsilon^\kappa\int_{\Omega_f}\mathcal{W}_f(\psi_{f,I})\; d\vec{x} \\ &\quad + \frac{\Delta t\; C_{p_m}}{2m_K}\sum_{j=1}^{2}\sum_{k=1}^{N}\|f_{m_j}^k\|_{\Omega_{m_j}}^2 + \varepsilon^{-\lambda}\frac{\Delta t\; C_{p_f}}{2m_K}\sum_{k=1}^{N}\|f_f^k\|_{\Omega_f}^2. \end{aligned} \tag{28}$$

Proof. We test in (22) with the triple $(\phi_{m_1}, \phi_{m_2}, \phi_f) = (\psi_{m_1}^k, \psi_{m_2}^k, \psi_f^k)$, which yields

$$\begin{aligned} &\sum_{j=1}^{2}(S_m(\psi_{m_j}^k) - S_m(\psi_{m_j}^{k-1}), \psi_{m_j}^k)_{\Omega_{m_j}} + \varepsilon^\kappa(S_f(\psi_f^k) - S_f(\psi_f^{k-1}), \psi_f^k)_{\Omega_f} \\ &\quad + \Delta t\sum_{j=1}^{2}(K_m(S_m(\psi_{m_j}^k))\nabla\psi_{m_j}^k, \nabla\psi_{m_j}^k)_{\Omega_{m_j}} + \varepsilon^\lambda\Delta t(K_f(S_f(\psi_f^k))\nabla\psi_f^k, \nabla\psi_f^k)_{\Omega_f} \\ &= \sum_{j=1}^{2}\Delta t(f_{m_j}^k, \psi_{m_j}^k)_{\Omega_{m_j}} + \Delta t(f_f^k, \psi_f^k)_{\Omega_f}. \end{aligned} \tag{29}$$

Poincaré's inequality gives

$$\|\nabla\psi_\rho^k\|_{\Omega_\rho}^2 \geq \frac{\|\nabla\psi_\rho^k\|_{\Omega_\rho}^2}{2} + \frac{\|\psi_\rho^k\|_{\Omega_\rho}^2}{2C_{p_\rho}}, \tag{30}$$

for $\rho \in \{m_1, m_2, f\}$, where $C_{p_\rho} > 0$ denotes the Poincaré constant of the respective subdomain. The geometries of Ω_{m_1} and Ω_{m_2} are the same, and so are the Poincaré

constants. Hence we set $C_{p_m} := C_{p_{m_1}} = C_{p_{m_2}}$, but note that for more general geometries, one can simply set $C_{p_m} := \max\{C_{p_{m_1}}, C_{p_{m_2}}\}$ in the following estimates.

Making use of this together with Assumption (A_K) and equation $(27)_2$ in Lemma 11, we estimate

$$\begin{aligned}
&\sum_{j=1}^{2}\int_{\Omega_{m_j}} \mathcal{W}_m(\psi_{m_j}^k)\ d\vec{x} + \varepsilon^\kappa \int_{\Omega_f} \mathcal{W}_f(\psi_f^k)\ d\vec{x} + \frac{\Delta t\ m_K}{2}\sum_{j=1}^{2}\|\nabla\psi_{m_j}^k\|_{\Omega_{m_j}}^2 \\
&+ \frac{\Delta t\ m_K}{2}\varepsilon^\lambda\|\nabla\psi_f^k\|_{\Omega_f}^2 + \frac{\Delta t\ m_K}{2C_{p_m}}\sum_{j=1}^{2}\|\psi_{m_j}^k\|_{\Omega_{m_j}}^2 + \varepsilon^\lambda\frac{\Delta t\ m_K\|\psi_f^k\|_{\Omega_f}^2}{2C_{p_f}} \\
&\le \sum_{j=1}^{2}\int_{\Omega_{m_j}} \mathcal{W}_m(\psi_{m_j}^{k-1})\ d\vec{x} + \varepsilon^\kappa \int_{\Omega_f} \mathcal{W}_f(\psi_f^{k-1})\ d\vec{x} + \frac{\Delta t\ C_{p_m}}{2m_K}\sum_{j=1}^{2}\|f_{m_j}^k\|_{\Omega_{m_j}}^2 + \\
&\varepsilon^{-\lambda}\frac{\Delta t\ C_{p_f}}{2m_K}\|f_f^k\|_{\Omega_f}^2 + \frac{\Delta t\ m_K}{2C_{p_m}}\sum_{j=1}^{2}\|\psi_{m_j}^k\|_{\Omega_{m_j}}^2 + \varepsilon^\lambda\frac{\Delta t\ m_K\|\psi_f^k\|_{\Omega_f}^2}{2C_{p_f}},
\end{aligned} \tag{31}$$

where we applied the Cauchy–Schwarz inequality and Young's inequality. Summing over k from 1 to l for an arbitrary $1 \le l \le N$ leaves us with

$$\begin{aligned}
&\sum_{j=1}^{2}\int_{\Omega_{m_j}} \mathcal{W}_m(\psi_{m_j}^l)\ d\vec{x} + \varepsilon^\kappa \int_{\Omega_f} \mathcal{W}_f(\psi_f^l)\ d\vec{x} + \frac{\Delta t\ m_K}{2}\sum_{j=1}^{2}\sum_{k=1}^{l}\|\nabla\psi_{m_j}^k\|_{\Omega_{m_j}}^2 \\
&+ \varepsilon^\lambda\frac{\Delta t\ m_K}{2}\sum_{k=1}^{l}\|\nabla\psi_f^k\|_{\Omega_f}^2 \le \sum_{j=1}^{2}\int_{\Omega_{m_j}} \mathcal{W}_m(\psi_{m_j,I})\ d\vec{x} + \varepsilon^\kappa \int_{\Omega_f} \mathcal{W}_f(\psi_{f,I})\ d\vec{x} \\
&+ \frac{\Delta t\ C_{p_m}}{2m_K}\sum_{j=1}^{2}\sum_{k=1}^{l}\|f_{m_j}^k\|_{\Omega_{m_j}}^2 + \varepsilon^{-\lambda}\frac{\Delta t\ C_{p_f}}{2m_K}\sum_{k=1}^{l}\|f_f^k\|_{\Omega_f}^2,
\end{aligned} \tag{32}$$

which finishes the proof. ∎

Remark 13. If other conditions are imposed at the outer boundaries and these are such that the Poincaré inequality does not hold in the form used, one may use the properties of $\mathcal{W}_\rho$ in (27) to obtain the a priori estimates. This gives then

$$\begin{aligned}
&\frac{1}{2}\sum_{j=1}^{2}\int_{\Omega_{m_j}} \mathcal{W}_m(\psi_{m_j}^l)\ d\vec{x} + \frac{1}{2}\varepsilon^\kappa \int_{\Omega_f} \mathcal{W}_f(\psi_f^l)\ d\vec{x} + \frac{m_S}{2}\sum_{j=1}^{2}\|\psi_{m_1}^l\|_{\Omega_{m_j}}^2 \\
&+ \frac{m_S}{2}\varepsilon^\kappa\|\psi_f^l\|_{\Omega_f}^2 + \frac{\Delta t\ m_K}{2}\sum_{j=1}^{2}\sum_{k=1}^{l}\|\nabla\psi_{m_j}^k\|_{\Omega_{m_j}}^2 + \varepsilon^\lambda\frac{\Delta t\ m_K}{2}\sum_{k=1}^{l}\|\nabla\psi_f^k\|_{\Omega_f}^2 \\
\le &\sum_{j=1}^{2}\int_{\Omega_{m_j}} \mathcal{W}_m(\psi_{m_j,I})\ d\vec{x} + \varepsilon^\kappa \int_{\Omega_f} \mathcal{W}_f(\psi_{f,I})\ d\vec{x} + \frac{\Delta t}{2m_S}\sum_{j=1}^{2}\sum_{k=1}^{l}\|f_{m_j}^k\|_{\Omega_{m_j}}^2 \\
&+ \varepsilon^{-\kappa}\frac{\Delta t}{2m_S}\sum_{k=1}^{l}\|f_f^k\|_{\Omega_f}^2 + \frac{\Delta t m_S}{2}\sum_{j=1}^{2}\sum_{k=1}^{l}\|\psi_{m_j}^k\|_{\Omega_{m_j}}^2 + \varepsilon^\kappa\frac{\Delta t m_S}{2}\sum_{k=1}^{l}\|\psi_f^k\|_{\Omega_f}^2,
\end{aligned}$$

and the rest follows by the discrete Gronwall lemma, but under additional assumptions on the source terms in the fractures.

Remark 14 (Non-degenerate case). In the strictly parabolic case as considered in this work, where an $m_S > 0$ exists such that $0 < m_S \leq S'_\rho(\psi_\rho)$ for all $\psi_\rho \in \mathbb{R}$, we immediately obtain an L^2 bound for ψ_ρ^k from the first two terms in Lemma 12 by Lemma 11:

$$m_S \frac{\|\psi_{m_j}^k\|^2_{\Omega_{m_j}}}{2} \leq \int_{\Omega_{m_j}} \mathcal{W}_m(\psi_{m_j}^k)\, d\vec{x}, \quad \text{and} \quad m_S \frac{\|\psi_f^k\|^2_{\Omega_f}}{2} \leq \int_{\Omega_f} \mathcal{W}_f(\psi_f^k)\, d\vec{x}. \tag{33}$$

In what follows, we prove the L^∞ stability of the time-discrete solution. We define the non-negative and non-positive cut of a function $u \in W^{1,2}(\Omega)$ by

$$[u]_+ := \max\{u, 0\}, \qquad [u]_- := \min\{u, 0\}. \tag{34}$$

Note that $[u]_+, [u]_- \in W^{1,2}(\Omega)$, see e.g. [30, Lemma 7.6].

LEMMA 15 (*A priori* estimate II). *For each* $\Delta t > 0$, $\rho \in \{m_1, m_2, f\}$, *and* $k \in \{1, \ldots, N\}$, *it holds*

$$\|\psi_\rho^k\|_{L^\infty(\Omega_\rho)} \leq M_\psi \left(k\Delta t + 1\right), \tag{35}$$

where

$$M_\psi := \max\left\{M_\rho, \frac{M_f}{m_S}\right\}. \tag{36}$$

Proof. The proof is done by induction. For $k = 0$, the statement holds due to Assumption (A_ρ). Assume now that $\|\psi_\rho^{k-1}\|_{L^\infty(\Omega_\rho)} < M_\psi\left((k-1)\Delta t + 1\right)$. First, we show that $\psi_\rho^k \leq M_\psi\left(k\Delta t + 1\right)$ almost everywhere in Ω_ρ.

We test equation (22) with $\phi_\rho = \left[\psi_\rho^k - M_\psi(k\Delta t + 1)\right]_+$. These test functions satisfy the required transmission condition because $\psi_{m_j}^k = \psi_f^k$ on Γ_j. Adding some terms on both sides of the equation, we obtain

$$\begin{aligned}
&\sum_{j=1}^{2} \left(S_m(\psi_{m_j}^k) - S_m\left(M_\psi(k\Delta t + 1)\right), \left[\psi_{m_j}^k - M_\psi(k\Delta t + 1)\right]_+ \right)_{\Omega_{m_j}} \\
&+ \varepsilon^\kappa \left(S_f(\psi_f^k) - S_f\left(M_\psi(k\Delta t + 1)\right), \left[\psi_f^k - M_\psi(k\Delta t + 1)\right]_+ \right)_{\Omega_f} \\
&+ \Delta t \sum_{j=1}^{2} \left(K_m(S_m(\psi_{m_j}^k)) \nabla \left(\psi_{m_j}^k - M_\psi(k\Delta t + 1)\right), \nabla \left[\psi_{m_j}^k - M_\psi(k\Delta t + 1)\right]_+ \right)_{\Omega_{m_j}} \\
&+ \varepsilon^\lambda \Delta t \left(K_f(S_f(\psi_f^k)) \nabla \left(\psi_f^k - M_\psi(k\Delta t + 1)\right), \nabla \left[\psi_f^k - M_\psi(k\Delta t + 1)\right]_+ \right)_{\Omega_f} \\
&= \sum_{j=1}^{2} \left(S_m(\psi_{m_j}^{k-1}) - S_m\left(M_\psi(k\Delta t + 1)\right), \left[\psi_{m_j}^k - M_\psi(k\Delta t + 1)\right]_+ \right)_{\Omega_{m_j}} \\
&+ \varepsilon^\kappa \left(S_f(\psi_f^{k-1}) - S_f\left(M_\psi(k\Delta t + 1)\right), \left[\psi_f^k - M_\psi(k\Delta t + 1)\right]_+ \right)_{\Omega_f} \\
&+ \Delta t \sum_{j=1}^{2} \left(f_{m_j}^k, \left[\psi_{m_j}^k - M_\psi(k\Delta t + 1)\right]_+ \right)_{\Omega_{m_j}} + \Delta t \left(f_f^k, \left[\psi_f^k - M_\psi(k\Delta t + 1)\right]_+ \right)_{\Omega_f}.
\end{aligned} \tag{37}$$

From Assumptions (A_S) and (A_K), and in particular the monotonicity of S_ρ, we deduce

$$
\begin{aligned}
& m_S \sum_{j=1}^{2} \left\| \left[\psi_{m_j}^k - M_\psi(k\Delta t+1)\right]_+ \right\|_{\Omega_{m_j}}^2 + \varepsilon^\kappa m_S \left\| \left[\psi_f^k - M_\psi(k\Delta t+1)\right]_+ \right\|_{\Omega_f}^2 \\
& + \Delta t\ m_K \sum_{j=1}^{2} \left\| \nabla \left[\psi_{m_j}^k - M_\psi(k\Delta t+1)\right]_+ \right\|_{\Omega_{m_j}}^2 \\
& + \varepsilon^\lambda \Delta t\ m_K \left\| \nabla \left[\psi_f^k - M_\psi(k\Delta t+1)\right]_+ \right\|_{\Omega_f}^2 \\
& \leq \sum_{j=1}^{2} \left(S_m(\psi_{m_j}^{k-1}) - S_m\left(M_\psi((k-1)\Delta t+1)\right), \left[\psi_{m_j}^k - M_\psi(k\Delta t+1)\right]_+ \right)_{\Omega_{m_j}} \\
& + \varepsilon^\kappa \left(S_f(\psi_f^{k-1}) - S_f\left(M_\psi((k-1)\Delta t+1)\right), \left[\psi_f^k - M_\psi(k\Delta t+1)\right]_+ \right)_{\Omega_f} \\
& + \Delta t \sum_{j=1}^{2} \left(\left(f_{m_j}^k - m_S M_\psi\right), \left[\psi_{m_j}^k - M_\psi(k\Delta t+1)\right]_+ \right)_{\Omega_{m_j}} \\
& + \Delta t \left(\left(f_f^k - m_S M_\psi\right), \left[\psi_f^k - M_\psi(k\Delta t+1)\right]_+ \right)_{\Omega_f}.
\end{aligned} \tag{38}
$$

On the right hand side above we used the inequality $S_\rho(\psi_\rho) \geq S_\rho(\xi_\rho) + m_S(\psi_\rho - \xi_\rho)$, valid if $\psi_\rho \geq \xi_\rho$, and yielding

$$
S_\rho\left(M_\psi((k\Delta t+1)\right) \geq S_\rho\left(M_\psi((k-1)\Delta t+1)\right) + m_S M_\psi \Delta t.
$$

Note that the first two terms on the right hand side in equation (38) are non-positive due to the induction assumption and the monotonicity of S_ρ. Since $M_\psi \geq \frac{M_f}{m_S}$, the last two terms are non-positive as well, from which we infer that $\psi_\rho^k \leq M_S(k\Delta t+1)$ almost everywhere in Ω_ρ. Similarly, one tests equation (22) with $\phi_\rho = \left[\psi_\rho^k + M_\psi(k\Delta t+1)\right]_-$ in order to show that $\psi_\rho^k \geq -M_\psi\left(k\Delta t+1\right)$ almost everywhere in Ω_ρ. This concludes the proof. ∎

4.7. Interpolation in time. Now, we define functions on a continuous time domain by interpolating the solutions of the time-discrete problem in time. We use piecewise linearly interpolated functions in addition to piecewise constant functions: for almost every $t \in (t_{k-1}, t_k]$ set

$$
\begin{aligned}
\bar{\Psi}_{\Delta t}^\rho(t) &:= \psi_\rho^k, \\
\bar{S}_{\Delta t}^\rho(t) &:= S(\psi_\rho^k), \\
\hat{S}_{\Delta t}^\rho(t) &:= S(\psi_\rho^{k-1}) + \frac{t-t_{k-1}}{\Delta t}(S(\psi_\rho^k) - S(\psi_\rho^{k-1})).
\end{aligned} \tag{39}
$$

Moreover, we need the piecewise constant interpolation of the source term $\bar{f}_{\Delta t}^\rho(t) = f_\rho^k$. In view of the *a priori* estimates in Lemmas 12 and 15, we obtain the following result for the interpolated functions:

LEMMA 16. *The functions $\bar{\Psi}_{\Delta t}^\rho$, $\bar{S}_{\Delta t}^\rho$, and $\hat{S}_{\Delta t}^\rho$ are bounded uniformly with respect to Δt in $L^\infty(0,T;L^2(\Omega_\rho)) \cap L^2(0,T;\mathcal{V}_\rho) \cap L^\infty(\Omega_\rho^T)$ for $\rho \in \{m_1, m_2, f\}$.*

In order to get a strong convergence in $L^2(0,T;L^2(\Omega_\rho))$, we need the following estimate for the time derivative of the saturation:

LEMMA 17. *Let $\kappa, \lambda \leq 0$ and assume that $\varepsilon^{-\lambda}\|f_f\|^2_{\Omega_f^T} \leq C$ and $\varepsilon^{\kappa}\int_{\Omega_f}\mathcal{W}(\psi_{f,I})\,d\vec{x} \leq C$. With $\rho \in \{m_1, m_2, f\}$, the functionals $\partial_t S_\rho$ are uniformly bounded w.r.t. ε in $L^2(0,T;W^{-1,2}(\Omega_\rho))$.*

Proof. We start with the formulation of the problem in the entire domain Ω, as stated in Definition 8. Further, using the time-interpolation in (39) and for any $\phi \in W_0^{1,2}(\Omega)$, for a.e. $t \in (0,T]$ one gets

$$
\begin{aligned}
\left|\langle \partial_t \hat{S}_{\Delta t}(t), \phi\rangle_{W^{-1,2}(\Omega),W_0^{1,2}(\Omega)}\right| &\leq \left|\left(K(S(\psi^k))\nabla\psi^k, \nabla\phi\right)_\Omega\right| + \left|\left(f^k, \phi\right)_\Omega\right| \\
&\leq M_K\left(\sum_{j=1}^{2}\|\nabla\phi_{m_j}\|_{\Omega_{m_j}}\|\nabla\psi^k_{m_j}\|_{\Omega_{m_j}} + \varepsilon^\lambda\|\nabla\phi_f\|_{\Omega_f}\|\nabla\psi^k_f\|_{\Omega_f}\right) \\
&\quad + \sum_{j=1}^{2}\|\phi_{m_j}\|_{\Omega_{m_j}}\|f^k_{m_j}\|_{\Omega_{m_j}} + \|\phi_f\|_{\Omega_f}\|f^k_f\|_{\Omega_f}, \\
&\leq \|\phi\|_{W^{1,2}(\Omega)}\left[M_K\left(\sum_{j=1}^{2}\|\nabla\psi^k_{m_j}\|_{\Omega_{m_j}} + \varepsilon^\lambda\|\nabla\psi^k_f\|_{\Omega_f}\right)\right. \\
&\quad \left. + \sum_{j=1}^{2}\|f^k_{m_j}\|_{\Omega_{m_j}} + \|f^k_f\|_{\Omega_f}\right],
\end{aligned}
\tag{40}
$$

where ϕ_ρ is the restriction of ϕ to Ω_ρ and we used the definition of K and S in (23). In view of the *a priori* estimate in Lemma 12 and using $\kappa, \lambda \leq 0$ and the assumptions on the source term and on the initial conditions, integrating in time gives

$$
\|\partial_t \hat{S}_{\Delta t}\|_{L^2(0,T;W^{-1,2}(\Omega))} \leq C, \tag{41}
$$

where C is independent of ε.

Recall the presence of a factor ε^κ in the definition of $\hat{S}$ in (23). To obtain an estimate on the subdomain Ω_f we consider the subspace of $W_0^{1,2}(\Omega)$ that consists of functions vanishing outside Ω_f, namely $\mathcal{W}_f^+ := \{\phi \in W_0^{1,2}(\Omega) : \phi = \chi_f\phi_f,\ \text{for } \phi_f \in W_0^{1,2}(\Omega_f)\}$. This bounds the $W^{-1,2}(\Omega_f)$ norm in terms of the $W^{-1,2}(\Omega)$ one,

$$
\begin{aligned}
\|\partial_t \hat{S}^f_{\Delta t}\|_{L^2(0,T;W^{-1,2}(\Omega_f))} &= \int_0^T \sup_{\phi_f \in W_0^{1,2}(\Omega_f),\phi_f\neq 0} \frac{|\langle \partial_t \hat{S}^f_{\Delta t}, \phi_f\rangle|_{W^{-1,2}(\Omega_f),W_0^{1,2}(\Omega_f)}}{\|\phi_f\|_{W^{1,2}(\Omega_f)}}\,dt \\
&\leq \varepsilon^{-\kappa}\int_0^T \sup_{\phi \in \mathcal{W}_f^+,\phi\neq 0} \frac{|\langle \partial_t \hat{S}_{\Delta t}, \phi\rangle|_{W^{-1,2}(\Omega),W_0^{1,2}(\Omega)}}{\|\phi\|_{W^{1,2}(\Omega)}}\,dt \\
&\leq \varepsilon^{-\kappa}\int_0^T \sup_{\phi \in W_0^{1,2}(\Omega),\phi\neq 0} \frac{|\langle \partial_t \hat{S}_{\Delta t}, \phi\rangle|_{W^{-1,2}(\Omega),W_0^{1,2}(\Omega)}}{\|\phi\|_{W^{1,2}(\Omega)}}\,dt \\
&= \varepsilon^{-\kappa}\|\partial_t \hat{S}_{\Delta t}\|^2_{L^2(0,T;W^{-1,2}(\Omega))} \leq C\varepsilon^{-\kappa}.
\end{aligned}
\tag{42}
$$

For $\kappa \leq 0$, this gives the desired estimate. ∎

Remark 18 ($\kappa, \lambda > 0$). If either κ or λ is greater than zero, the proof of Lemma 17 can be repeated but the constant C is no longer uniform w.r.t. ε. Nonetheless, $\partial_t S_\rho$ remains bounded in $L^2(0,T;W^{-1,2}(\Omega_\rho))$, $\rho \in \{m_1, m_2, f\}$, for each fixed $\varepsilon > 0$.

Compactness arguments give rise to the following convergent subsequences:

LEMMA 19. *There exists a* $\Psi_\rho \in L^2(0,T;\mathcal{V}_\rho)$ *and a subsequence* $\Delta t \to 0$ *along which we obtain for* $\rho \in \{m_1, m_2, f\}$

$$
\begin{aligned}
&\{\hat{S}^\rho_{\Delta t}\}_{\Delta t} \to S_\rho(\Psi_\rho) && \text{strongly in } L^2(0,T;L^2(\Omega_\rho)),\\
&\{\bar{S}^\rho_{\Delta t}\}_{\Delta t} \to S_\rho(\Psi_\rho) && \text{strongly in } L^2(0,T;L^2(\Omega_\rho)),\\
&\{\bar{\Psi}^\rho_{\Delta t}\}_{\Delta t} \to \Psi_\rho && \text{strongly in } L^2(0,T;L^2(\Omega_\rho)),\\
&\{\bar{\Psi}^\rho_{\Delta t}\}_{\Delta t} \rightharpoonup \Psi_\rho && \text{weakly in } L^2(0,T;\mathcal{V}_\rho).
\end{aligned}
\tag{43}
$$

Proof. The first convergence follows from the Aubin–Lions–Simon theorem [9, 65] by the estimates in Lemmas 16 and 17 (also see Remark 18). The convergence of the piecewise linearly interpolated functions implies the convergence of the piecewise constantly interpolated functions towards the same limit function (see e.g. [42, Lemma 3.2]). The third convergence is a consequence of Assumption (A_S) ensuring that the inverse function S_ρ^{-1} exists and is Lipschitz continuous. Finally, the weak convergence in $L^2(0,T;\mathcal{V}_\rho)$ is provided by the Eberlein–Šmulian theorem in view of the bounds in Lemma 16. ∎

It remains to show that the triple of limit functions is a weak solution:

THEOREM 20. *The limit* $(\Psi_{m_1}, \Psi_{m_2}, \Psi_f)$ *is a weak solution to Problem* $\mathcal{P}_\varepsilon$ *in the sense of Definition 4.*

Proof. Let $(\phi_{m_1}, \phi_{m_2}, \phi_f) \in \mathcal{V}_{m_1} \times \mathcal{V}_{m_2} \times \mathcal{V}_f$. Summing (22) from 1 to k yields for almost every $t \in (t_{k-1}, t_k)$

$$
\begin{aligned}
&\sum_{j=1}^{2} \left(S_m(\bar{\Psi}^{m_j}_{\Delta t}(t)), \phi_{m_j}\right)_{\Omega_{m_j}} + \varepsilon^\kappa \left(S_f(\bar{\Psi}^f_{\Delta t}(t)), \phi_f\right)_{\Omega_f}\\
&\quad - \sum_{j=1}^{2} \left(S_m(\psi_{m_j,I}), \phi_{m_j}\right)_{\Omega_{m_j}} - \varepsilon^\kappa \left(S_f(\psi_{f,I}), \phi_f\right)_{\Omega_f}\\
&\quad + \sum_{j=1}^{2} \int_0^t \left(K_m(S_m(\bar{\Psi}^{m_j}_{\Delta t}(\tau)))\nabla \bar{\Psi}^{m_j}_{\Delta t}(\tau), \nabla\phi_{m_j}\right)_{\Omega_{m_j}} d\tau\\
&\quad + \varepsilon^\lambda \int_0^t \left(K_f(S_f(\bar{\Psi}^f_{\Delta t}(\tau)))\nabla \bar{\Psi}^f_{\Delta t}(\tau), \nabla\phi_f\right)_{\Omega_f} d\tau\\
&\quad - \sum_{j=1}^{2} \int_0^t \left(\bar{f}_{m_j}(\tau), \phi_{m_j}\right)_{\Omega_{m_j}} d\tau - \int_0^t \left(\bar{f}_f(\tau), \phi_f\right)_{\Omega_f} d\tau\\
=&\sum_{j=1}^{2} \int_t^{t_k} \left(\bar{f}_{m_j}(\tau), \phi_{m_j}\right)_{\Omega_{m_j}} d\tau + \int_t^{t_k} \left(\bar{f}_f(\tau), \phi_f\right)_{\Omega_f} d\tau\\
&\quad - \sum_{j=1}^{2} \int_t^{t_k} \left(K_m(S_m(\bar{\Psi}^{m_j}_{\Delta t}(\tau)))\nabla \bar{\Psi}^{m_j}_{\Delta t}(\tau), \nabla\phi_{m_j}\right)_{\Omega_{m_j}} d\tau\\
&\quad - \varepsilon^\lambda \int_t^{t_k} \left(K_f(S_f(\bar{\Psi}^f_{\Delta t}(\tau)))\nabla \bar{\Psi}^f_{\Delta t}(\tau), \nabla\phi_f\right)_{\Omega_f} d\tau.
\end{aligned}
\tag{44}
$$

The terms on the right hand side correct the error made on the left hand side by integrating to t instead of t_k. Now, we choose test functions $(\phi_{m_1}, \phi_{m_2}, \phi_f) \in$

$L^2(0,T;\mathcal{V}_{m_1}) \times L^2(0,T;\mathcal{V}_{m_2}) \times L^2(0,T;\mathcal{V}_f)$ fulfilling $\phi_{m_j} = \phi_f$ on Γ_j and integrate in time from 0 to T to get

(45)

$$\begin{aligned}
&\sum_{j=1}^{2}\int_0^T \big(S_m(\bar{\Psi}^{m_j}_{\Delta t}(t)),\phi_{m_j}(t)\big)_{\Omega_{m_j}}\,dt + \varepsilon^{\kappa}\int_0^T \Big(S_f(\bar{\Psi}^{f}_{\Delta t}(t)),\phi_f(t)\Big)_{\Omega_f}\,dt\\
&-\sum_{j=1}^{2}\int_0^T \big(S_m(\psi_{m_j,I}),\phi_{m_j}(t)\big)_{\Omega_{m_j}}\,dt - \varepsilon^{\kappa}\int_0^T (S_f(\psi_{f,I}),\phi_f(t))_{\Omega_f}\,dt\\
&+\sum_{j=1}^{2}\int_0^T\int_0^t \big(K_m(S_m(\bar{\Psi}^{m_j}_{\Delta t}(\tau)))\nabla\bar{\Psi}^{m_j}_{\Delta t}(\tau),\nabla\phi_{m_j}(t)\big)_{\Omega_{m_j}}\,d\tau\,dt\\
&+\varepsilon^{\lambda}\int_0^T\int_0^t \Big(K_f(S_f(\bar{\Psi}^{f}_{\Delta t}(\tau)))\nabla\bar{\Psi}^{f}_{\Delta t}(\tau),\nabla\phi_f(t)\Big)_{\Omega_f}\,d\tau\,dt\\
&-\sum_{j=1}^{2}\int_0^T\int_0^t \big(\bar{f}_{m_j}(\tau),\phi_{m_j}(t)\big)_{\Omega_{m_j}}\,d\tau\,dt - \int_0^T\int_0^t \big(\bar{f}_f(\tau),\phi_f(t)\big)_{\Omega_f}\,d\tau\,dt\\
&=\sum_{j=1}^{2}\sum_{k=1}^{N}\int_{t_{k-1}}^{t_k}\int_t^{t_k} \big(\bar{f}_{m_j}(\tau),\phi_{m_j}(t)\big)_{\Omega_{m_j}}\,d\tau\,dt + \sum_{k=1}^{N}\int_{t_{k-1}}^{t_k}\int_t^{t_k} \big(\bar{f}_f(\tau),\phi_f(t)\big)_{\Omega_f}\,d\tau\,dt\\
&-\sum_{j=1}^{2}\sum_{k=1}^{N}\int_{t_{k-1}}^{t_k}\int_t^{t_k} \big(K_m(S_m(\bar{\Psi}^{m_j}_{\Delta t}(\tau)))\nabla\bar{\Psi}^{m_j}_{\Delta t}(\tau),\nabla\phi_{m_j}(t)\big)_{\Omega_{m_j}}\,d\tau\,dt\\
&-\varepsilon^{\lambda}\sum_{k=1}^{N}\int_{t_{k-1}}^{t_k}\int_t^{t_k} \Big(K_f(S_f(\bar{\Psi}^{f}_{\Delta t}(\tau)))\nabla\bar{\Psi}^{f}_{\Delta t}(\tau),\nabla\phi_f(t)\Big)_{\Omega_f}\,d\tau\,dt.
\end{aligned}$$

From the strong L^2 convergence in $(43)_2$, we infer that

$$\int_0^T \big(S_\rho(\bar{\Psi}^{\rho}_{\Delta t}(t)),\phi_\rho(t)\big)_{\Omega_\rho}\,dt \to \int_0^T (S_\rho(\Psi_\rho(t)),\phi_\rho(t))_{\Omega_\rho}\,dt. \tag{46}$$

Furthermore, the strong convergence of $\bar{\Psi}^{\rho}_{\Delta t}$ in $L^2(0,T;L^2(\Omega_\rho))$ in equation $(43)_3$ and the weak convergence of the gradients in $L^2(0,T;L^2(\Omega_\rho))$ in equation $(43)_4$ together with the Lipschitz continuity of S_ρ and K_ρ yield

$$\begin{aligned}
&\int_0^T\int_0^t \big(K_\rho(S_\rho(\bar{\Psi}^{\rho}_{\Delta t}(\tau)))\nabla\bar{\Psi}^{\rho}_{\Delta t}(\tau),\nabla\phi_\rho(t)\big)_{\Omega_\rho}\,d\tau\,dt\\
&\qquad\to\int_0^T\int_0^t (K_\rho(S_\rho(\Psi_\rho(\tau)))\nabla\Psi_\rho(\tau),\nabla\phi_\rho(t))_{\Omega_\rho}\,d\tau\,dt.
\end{aligned} \tag{47}$$

This follows from the following considerations: due to the ellipticity of K_ρ, $\bar{\Psi}^{\rho}_{\Delta t}$ converges strongly in $L^2(0,T;L^2(\Omega_\rho))$ and because of the Lipschitz continuity of K_ρ and S_ρ, $K_\rho(S_\rho(\bar{\Psi}^{\rho}_{\Delta t}(\tau)))$ converges to $K_\rho(S_\rho(\Psi_\rho(\tau)))$ strongly in $L^2(0,T;L^2(\Omega_\rho))$. The boundedness of K_ρ gives the existence of a $\vec{\xi}_\rho \in L^2(0,T;\big(L^2(\Omega_\rho)\big)^d)$ such that

$$\int_0^t K_\rho(S_\rho(\bar{\Psi}^{\rho}_{\Delta t}(\tau)))\nabla\bar{\Psi}^{\rho}_{\Delta t}(\tau)d\tau \rightharpoonup \vec{\xi}_\rho, \qquad \text{weakly in } L^2(0,T;\big(L^2(\Omega_\rho)\big)^d). \tag{48}$$

The identification of $\vec{\xi}_\rho$ to $K_\rho(S_\rho(\Psi_\rho))\nabla\Psi_\rho$ then follows by taking smoother test functions in (47) and passing to the limit.

Moreover, the time-continuity of f gives

$$\int_0^T \int_0^t \left(\bar{f}_\rho(\tau), \phi_\rho(t)\right)_{\Omega_\rho} d\tau \; dt \to \int_0^T \int_0^t \left(f_\rho(\tau), \phi_\rho(t)\right)_{\Omega_\rho} d\tau \; dt. \tag{49}$$

In what follows, we show that the terms on the right hand side in equation (45) vanish as Δt approaches zero. For the terms involving a source term f_ρ, we obtain

$$\left| \sum_{k=1}^N \int_{t_{k-1}}^{t_k} \int_t^{t_k} \left(\bar{f}_\rho(\tau), \phi_\rho(t)\right)_{\Omega_\rho} d\tau \; dt \right| \leq \frac{(\Delta t)^2}{2} \sum_{k=1}^N \|f_\rho^k\|^2_{\Omega_\rho} + \frac{\Delta t}{2} \int_0^T \|\phi_\rho\|^2_{\Omega_\rho} \leq C\Delta t, \tag{50}$$

where we used the Cauchy–Schwarz inequality and Young's inequality. Furthermore, we get

$$\begin{aligned} &\left| \sum_{k=1}^N \int_{t_{k-1}}^{t_k} \int_t^{t_k} \left(K_\rho(S_\rho(\bar{\Psi}^\rho_{\Delta t}(\tau)))\nabla \bar{\Psi}^\rho_{\Delta t}(\tau), \nabla \phi_\rho(t)\right)_{\Omega_\rho} d\tau \; dt \right| \\ \leq &\frac{(\Delta t)^2 M_K}{2} \sum_{k=1}^N \|\nabla \psi_\rho^k\|^2_{\Omega_\rho} + \frac{\Delta t}{2} \int_0^T \|\nabla \phi_\rho\|^2_{\Omega_\rho} \leq C\Delta t, \end{aligned} \tag{51}$$

using the *a priori* estimate in Lemma 12. Therefore letting $\Delta t \to 0$ gives

$$\begin{aligned} &\sum_{j=1}^2 \int_0^T \left(S_m(\Psi_{m_j}(t)), \phi_{m_j}(t)\right)_{\Omega_{m_j}} dt + \varepsilon^\kappa \int_0^T \left(S_f(\Psi_f(t)), \phi_f(t)\right)_{\Omega_f} dt \\ &+ \sum_{j=1}^2 \int_0^T \int_0^t \left(K_m(S_m(\Psi_{m_j}(\tau)))\nabla \Psi_{m_j}(\tau), \nabla \phi_{m_j}(t)\right)_{\Omega_{m_j}} d\tau \; dt \\ &+ \varepsilon^\lambda \int_0^T \int_0^t \left(K_f(S_f(\Psi_f(\tau)))\nabla \Psi_{m_j}(\tau), \nabla \phi_f(t)\right)_{\Omega_f} d\tau \; dt \\ = &\sum_{j=1}^2 \int_0^T \int_0^t \left(f_{m_j}(\tau), \phi_{m_j}(t)\right)_{\Omega_{m_j}} d\tau \; dt + \int_0^T \int_0^t \left(f_f(\tau), \phi_f(t)\right)_{\Omega_f} d\tau \; dt \\ &+ \sum_{j=1}^2 \int_0^T \left(S_m(\psi_{m_j,I}), \phi_{m_j}(t)\right)_{\Omega_{m_j}} dt + \varepsilon^\kappa \int_0^T \left(S_f(\psi_{f,I}), \phi_f(t)\right)_{\Omega_f} dt, \end{aligned} \tag{52}$$

for all $(\phi_{m_1}, \phi_{m_2}, \phi_f) \in L^2(0,T;\mathcal{V}_{m_1}) \times L^2(0,T;\mathcal{V}_{m_2}) \times L^2(0,T;\mathcal{V}_f)$ such that $\phi_{m_j} = \phi_f$ on Γ_j for $j \in \{1,2\}$.

Note that for test functions $(\tilde{\phi}_{m_1}, \tilde{\phi}_{m_2}, \tilde{\phi}_f) \in W^{1,2}(0,T;\mathcal{V}_{m_1}) \times W^{1,2}(0,T;\mathcal{V}_{m_2}) \times W^{1,2}(0,T;\mathcal{V}_f)$ satisfying $\tilde{\phi}_{m_1}(T) = \tilde{\phi}_{m_2}(T) = \tilde{\phi}_f(T) = 0$, integration by parts yields

$$\begin{aligned} &\int_0^T \int_0^t \left(f_\rho(\tau), \partial_t \tilde{\phi}_\rho(t)\right)_{\Omega_\rho} d\tau \; dt = -\int_0^T \left(f_\rho(t), \tilde{\phi}_\rho(t)\right)_{\Omega_\rho} dt, \\ &\int_0^T \int_0^t \left(K_\rho(S_\rho(\Psi_\rho(\tau)))\nabla \Psi_\rho(\tau), \nabla \partial_t \tilde{\phi}_\rho(t)\right)_{\Omega_\rho} d\tau \; dt \\ &= -\int_0^T \left(K_\rho(S_\rho(\Psi_\rho(t)))\nabla \Psi_\rho(t), \nabla \tilde{\phi}_\rho(t)\right)_{\Omega_\rho} dt. \end{aligned} \tag{53}$$

Thus, selecting $\phi_\rho = \partial_t \tilde{\phi}_\rho$ in (52) gives

$$
\begin{aligned}
&\sum_{j=1}^{2} \int_0^T \left(S_m(\Psi_{m_j}(t)), \partial_t \tilde{\phi}_{m_j}(t) \right)_{\Omega_{m_j}} dt + \varepsilon^\kappa \int_0^T \left(S_f(\Psi_f(t)), \partial_t \tilde{\phi}_f(t) \right)_{\Omega_f} dt \\
&- \sum_{j=1}^{2} \int_0^T \left(K_m(S_m(\Psi_{m_j}(t))) \nabla \Psi_{m_j}(t), \nabla \tilde{\phi}_{m_j}(t) \right)_{\Omega_{m_j}} dt \\
&- \varepsilon^\lambda \int_0^T \left(K_f(S_f(\Psi_f(t))) \nabla \Psi_{m_j}(t), \nabla \tilde{\phi}_f(t) \right)_{\Omega_f} dt \\
&= - \sum_{j=1}^{2} \int_0^T \left(f_{m_j}(t), \tilde{\phi}_{m_j}(t) \right)_{\Omega_{m_j}} dt - \int_0^T \left(f_f(t), \tilde{\phi}_f(t) \right)_{\Omega_f} dt \\
&- \sum_{j=1}^{2} \left(S_m(\psi_{m_j,I}), \tilde{\phi}_{m_j}(0) \right)_{\Omega_{m_j}} - \varepsilon^\kappa \left(S_f(\psi_{f,I}), \tilde{\phi}_f(0) \right)_{\Omega_f}.
\end{aligned} \tag{54}
$$

Therefore, equation (18) holds true for all appropriate test functions.
In order to show that the interface conditions are satisfied, we estimate

$$
\|\Psi_{m_j} - \Psi_f\|_{\Gamma_j^T} \leq \|\Psi_{m_j} - \bar{\Psi}_{\Delta t}^{m_j}\|_{\Gamma_j^T} + \|\bar{\Psi}_{\Delta t}^{m_j} - \bar{\Psi}_{\Delta t}^{f}\|_{\Gamma_j^T} + \|\bar{\Psi}_{\Delta t}^{f} - \Psi_f\|_{\Gamma_j^T} \tag{55}
$$

and consider the terms on the right hand side individually. The second term is zero by the definition of the time-discrete weak solution. For the first term, the trace inequality gets

$$
\begin{aligned}
&\|\Psi_{m_j} - \bar{\Psi}_{\Delta t}^{m_j}\|_{\Gamma_j^T}^2 \\
&\leq C(\Omega_{m_j}) \|\Psi_{m_j} - \bar{\Psi}_{\Delta t}^{m_j}\|_{\Omega_{m_j}^T} \left(\|\nabla \Psi_{m_j} - \nabla \bar{\Psi}_{\Delta t}^{m_j}\|_{\Omega_{m_j}^T} + \|\Psi_{m_j} - \bar{\Psi}_{\Delta t}^{m_j}\|_{\Omega_{m_j}^T} \right).
\end{aligned} \tag{56}
$$

By the weak convergence in equation $(43)_4$, the term in brackets is bounded, and from the strong convergence in equation $(43)_3$, we get that $\|\Psi_{m_j} - \bar{\Psi}_{\Delta t}^{m_j}\|_{\Omega_{m_j}^T} \to 0$ for $\Delta t \to 0$. The third term on the right hand side of equation (55) vanishes with an analogous argument, which finishes the proof. ∎

Remark 21. For fixed ε, the estimate in the fracture can be improved by isolating the equation in the fracture. By carrying out the same procedure as above but with $\phi_f \in L^2(0,T;W_0^{1,2}(\Omega_f))$, that is, having zero boundary values on Ω_f, we obtain

$$
\begin{aligned}
\partial_t \hat{S}_{\Delta t} &\rightharpoonup \partial_t S_f(\psi_f) && \text{weakly in } L^2(0,T;W^{-1,2}(\Omega_f)), \\
K_f(S_f(\bar{\Psi}_{\Delta t}^f)) \nabla \bar{\Psi}_{\Delta t}^f &\rightharpoonup K_f(S_f(\psi_f)) \nabla \psi_f && \text{weakly in } L^2(0,T;\left(L^2(\Omega_f)\right)^d),
\end{aligned} \tag{57}
$$

and ψ_f satisfies the equation,

$$
\varepsilon^\kappa \left(\partial_t S_f(\psi_f), \phi_f \right)_{\Omega_f^T} + \varepsilon^\lambda \left(K_f(S_f(\psi_f)) \nabla \psi_f, \nabla \phi_f \right)_{\Omega_f^T} = \left(f_f, \phi_f \right)_{\Omega_f^T}, \tag{58}
$$

for all $\phi_f \in L^2(0,T;W_0^{1,2}(\Omega_f))$.

5. Rigorous upscaling. In this section, we give the rigorous proof of the upscaling result, namely the convergence of the solution to Problem $\mathcal{P}_\varepsilon$ towards the solution to the effective models in the limit $\varepsilon \to 0$. We present the upscaling for the parameter

range $(\kappa, \lambda) \in [-1, \infty) \times (-\infty, 1)$ except for the case when $\kappa = -1, \lambda \in (-1, 1)$. This corresponds to scenarios in which the fracture-to-matrix porosity ratio does not grow too fast and the fracture-to-matrix conductivity ratio only decreases moderately in terms of ε.

We employ techniques from [20], where upscaling was considered in the context of crystal dissolution and precipitation, and [57], which is concerned with the upscaling of a reactive transport model. For a more detailed presentation of the results, we refer the reader to [43].

5.1. Kirchhoff transformation and rescaling of the geometry. We apply the Kirchhoff transform (see [4]) in each subdomain. For this, we introduce a function

$$\mathcal{K}_\rho : \mathbb{R} \to \mathbb{R}, \qquad u_\rho := \mathcal{K}_\rho(\psi_\rho) = \int_0^{\psi_\rho} K_\rho(S_\rho(\varphi))\, d\varphi. \tag{59}$$

Due to the assumptions on K_ρ and S_ρ, the Kirchhoff transformation is invertible and one can define the function

$$b_\rho(u_\rho) := S_\rho \circ \mathcal{K}_\rho^{-1}(u_\rho). \tag{60}$$

Note that b_ρ is Lipschitz continuous due to the Lipschitz continuity of S_ρ and $\mathcal{K}_\rho^{-1}$. By the chain rule, one obtains $\nabla u_\rho = K_\rho(S_\rho(\psi_\rho))\nabla\psi_\rho$, which transforms Problem $\mathcal{P}_\varepsilon$ into a semi-linear problem. Since $\mathcal{K}_\rho$ is Lipschitz continuous, the Kirchhoff transformed problem is equivalent to the original problem [45], and all *a priori* estimates from the previous section are satisfied for the Kirchhoff transformed variables, too. The advantage of the Kirchhoff transformed formulation is the linear flux term. However, this comes at the cost of a nonlinear transmission condition for the Kirchhoff transformed pressure variable.

We rescale the fracture in horizontal direction by defining $z = x/\varepsilon$, and consider the following

$$\begin{aligned} \tilde{u}_f(t, z, y) &= u_f(t, z\varepsilon, y), \\ \tilde{u}_{f,I}(z, y) &= u_{f,I}(z\varepsilon, y) := \mathcal{K}_f(\psi_{f,I})(z\varepsilon, y), \\ \tilde{f}_f(t, z, y) &= f_f(t, z\varepsilon, y). \end{aligned} \tag{61}$$

To unify the notation, we set $z = x$ in the matrix blocks. Observe that this means practically that the solid matrix subdomains are merely translated w.r.t. ε. Since they do not change their shape, we omit the ε in the notation and still write Ω_{m_j}. For the fracture model instead the ε dependence is explicit. We use $\Omega_f^\varepsilon := (-\frac{\varepsilon}{2}, \frac{\varepsilon}{2}) \times (0, 1)$ in this section, and the shorthand notation $\Omega_f := \Omega_f^1$. Observe that this is also the domain for the rescaled pair of variables (z, y). The solution in each domain, u_ρ^ε, will be endowed with a superscript ε to emphasise the ε-dependence.

The fracture solutions in the effective models are defined on the reduced-dimensional fracture, $\Gamma = \{0\} \times (0, 1)$. For the weak solution we define the function spaces

$$\bar{\mathcal{V}}_f := \{u \in L^2(\Gamma) : \partial_y u \in L^2(\Gamma), u = 0 \text{ on } \partial\Gamma\} = W_0^{1,2}(\Gamma). \tag{62}$$

Figure 2 illustrates the geometry of the problem in rescaled variables and the geometry of the effective models, in which the fracture has become one-dimensional.

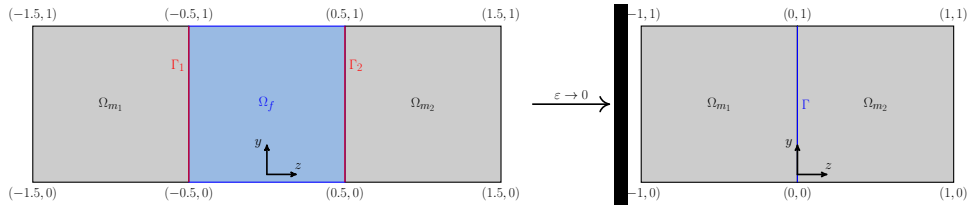

FIG. 2. *Geometry with two-dimensional fracture in rescaled variables (left) and upscaled geometry with one-dimensional fracture (right)*

For each $\varepsilon > 0$, we define the z-averaged quantities

(63)
$$\bar{u}_f^\varepsilon(t,y) := \int_{-\frac{1}{2}}^{\frac{1}{2}} \tilde{u}_f^\varepsilon(t,z,y)\ dz, \qquad \bar{f}_f(t,y) := \int_{-\frac{1}{2}}^{\frac{1}{2}} \tilde{f}_f(t,z,y)\ dz,$$
$$\bar{b}_f(\tilde{u}_f^\varepsilon)(t,y) := \int_{-\frac{1}{2}}^{\frac{1}{2}} b_f(\tilde{u}_f^\varepsilon)(t,z,y)\ dz, \qquad \bar{b}_f(\tilde{u}_{f,I}^\varepsilon)(y) := \int_{-\frac{1}{2}}^{\frac{1}{2}} b_f(\tilde{u}_{f,I}^\varepsilon)(z,y)\ dz,$$

as well as

(64)
$$\breve{u}_f^\varepsilon(t) := \int_0^1 \bar{u}_f^\varepsilon(t,y)\ dy, \qquad \breve{f}_f(t) = \int_0^1 \bar{f}_f(t,y)\ dy,$$
$$\breve{b}_f(\tilde{u}_f^\varepsilon)(t) := \int_0^1 \bar{b}_f(\tilde{u}_f^\varepsilon)(t,y)\ dy, \qquad \breve{b}_f(\tilde{u}_{f,I}^\varepsilon) := \int_0^1 \bar{b}_f(\tilde{u}_{f,I})(y)\ dy.$$

We state the weak formulation in terms of the Kirchhoff transformed and rescaled variables. In terms of the rescaled variables, the geometry is ε-independent and the x-argument of the functions associated with the fracture becomes ε-dependent instead:

DEFINITION 22 (Weak solution in rescaled variables). *A triple* $(u_{m_1}^\varepsilon, u_{m_2}^\varepsilon, \tilde{u}_f^\varepsilon) \in L^2(0,T;\mathcal{V}_{m_1}) \times L^2(0,T;\mathcal{V}_{m_2}) \times L^2(0,T;\mathcal{V}_f)$ *is called a weak solution to the Kirchhoff transformed formulation of Problem* $\mathcal{P}_\varepsilon$ *if*

(65)
$$\mathcal{K}_m^{-1}(u_{m_1}^\varepsilon) = \mathcal{K}_f^{-1}(\tilde{u}_f^\varepsilon) \quad \text{on } \Gamma_1 \text{ and} \quad \mathcal{K}_m^{-1}(u_{m_2}^\varepsilon) = \mathcal{K}_f^{-1}(\tilde{u}_f^\varepsilon) \quad \text{on } \Gamma_2 \text{ for a.e. } t \in [0,T],$$

in the sense of traces, and

(66)
$$\begin{aligned}
&-\sum_{j=1}^{2} \left(b_m(u_{m_j}^\varepsilon), \partial_t \phi_{m_j}\right)_{\Omega_{m_j}^T} - \varepsilon^{\kappa+1} \left(b_f(\tilde{u}_f^\varepsilon), \partial_t \phi_f\right)_{\Omega_f^T} \\
&+\sum_{j=1}^{2} \left(\nabla u_{m_j}^\varepsilon, \nabla \phi_{m_j}\right)_{\Omega_{m_j}^T} + \varepsilon^{\lambda-1} \left(\partial_z \tilde{u}_f^\varepsilon, \partial_z \phi_f\right)_{\Omega_f^T} + \varepsilon^{\lambda+1} \left(\partial_y \tilde{u}_f^\varepsilon, \partial_y \phi_f\right)_{\Omega_f^T} \\
&= \sum_{j=1}^{2} \left(f_{m_j}, \phi_{m_j}\right)_{\Omega_{m_j}^T} + \varepsilon \left(\tilde{f}_f, \phi_f\right)_{\Omega_f^T} \\
&+\sum_{j=1}^{2} \left(b_m(u_{m_j,I}), \phi_{m_j}(0)\right)_{\Omega_{m_j}} + \varepsilon^{\kappa+1} \left(b_f(\tilde{u}_{f,I}), \phi_f(0)\right)_{\Omega_f},
\end{aligned}$$

for all $(\phi_{m_1}, \phi_{m_2}, \phi_f) \in W^{1,2}(0,T;\mathcal{V}_{m_1}) \times W^{1,2}(0,T;\mathcal{V}_{m_2}) \times W^{1,2}(0,T;\mathcal{V}_f)$ *satisfying*

(67)
$$\phi_{m_1} = \phi_f \quad \text{on } \Gamma_1 \quad \text{and} \quad \phi_{m_2} = \phi_f \quad \text{on } \Gamma_2 \quad \text{for a.e. } t \in [0,T],$$

and

$$\phi_\rho(T) = 0 \qquad \text{for } \rho \in \{m_1, m_2, f\}. \tag{68}$$

The formulation in Definition 22 is the starting point for deriving limit models for all choices of κ and λ.

5.2. Uniform estimates with respect to ε. In order to prove the convergence of Problem $\mathcal{P}_\varepsilon$ towards an effective model, we establish estimates for the solution and its derivatives independent of ε, similar to the uniform estimates with respect to Δt in Section 4.

Testing with z-independent functions $\phi_f(t,z,y) = \phi_f(t,y)$ in the fracture (and hence ϕ_{m_1} and ϕ_{m_2} fulfilling $\phi_{m_1}(t,z,y)|_{\Gamma_1} = \phi_f(t,y) = \phi_{m_2}(t,z,y)|_{\Gamma_2}$ for a.e. $t \in [0,T]$) in Definition 22 gives

$$\begin{aligned} &-\sum_{j=1}^{2}\Big(b_m(u^\varepsilon_{m_j}),\partial_t\phi_{m_j}\Big)_{\Omega^T_{m_j}} - \varepsilon^{\kappa+1}(\bar b_f(\tilde u^\varepsilon_f),\partial_t\phi_f)_{\Gamma^T} + \sum_{j=1}^{2}\Big(\nabla u^\varepsilon_{m_j},\nabla\phi_{m_j}\Big)_{\Omega^T_{m_j}} \\ &+\varepsilon^{\lambda+1}(\partial_y\bar u^\varepsilon_f,\partial_y\phi_f)_{\Gamma^T} = \sum_{j=1}^{2}\big(f_{m_j},\phi_{m_j}\big)_{\Omega^T_{m_j}} + \varepsilon(\bar f_f,\phi_f)_{\Gamma^T} \\ &+\sum_{j=1}^{2}\big(b_m(u_{m_j,I}),\phi_{m_j}(0)\big)_{\Omega_{m_j}} + \varepsilon^{\kappa+1}\left(\bar b_f(\tilde u_{f,I}),\phi_f(0)\right)_\Gamma, \end{aligned} \tag{69}$$

for all $(\phi_{m_1},\phi_{m_2},\phi_f) \in W^{1,2}(0,T;\mathcal{V}_{m_1}) \times W^{1,2}(0,T;\mathcal{V}_{m_2}) \times W^{1,2}(0,T;\bar{\mathcal{V}}_f)$ satisfying $\phi_{m_1}(t,z,y)|_{\Gamma_1} = \phi_f(t,y) = \phi_{m_2}(t,z,y)|_{\Gamma_2}$ for a.e. $t \in [0,T]$ and $\phi_\rho(T) = 0$ for $\rho \in \{m_1,m_2,f\}$.

Based on the *a priori* estimate in Lemma 12, one shows that the solution and its derivatives can be bounded uniformly in ε for $\kappa \geq -1$, $\lambda \leq -1$, and $\varepsilon > 0$ sufficiently small. In addition, we get uniform essential bounds for the solution since the constant M_ψ in Lemma 15 is ε-independent:

LEMMA 23. *There exists a $C > 0$ independent of ε such that*

$$\begin{aligned} &\sum_{j=1}^{2}\|u^\varepsilon_{m_j}\|^2_{L^2(0,T;\mathcal{V}_{m_j})} + \varepsilon^{\kappa+1}\|\tilde u^\varepsilon_f\|^2_{\Omega^T_f} + \varepsilon^{\lambda+1}\|\partial_y\tilde u^\varepsilon_f\|^2_{\Omega^T_f} + \varepsilon^{\lambda-1}\|\partial_z\tilde u^\varepsilon_f\|^2_{\Omega^T_f} \leq C, \\ &\sum_{j=1}^{2}\|u^\varepsilon_{m_j}\|_{L^\infty(\Omega^T_{m_j})} + \|\tilde u^\varepsilon_f\|_{L^\infty(\Omega^T_f)} \leq C. \end{aligned} \tag{70}$$

These estimates are directly carried over to the averages of fracture solution by virtue of Jensen's inequality:

LEMMA 24. *There exists a $C > 0$ independent of ε such that*

$$\varepsilon^{\kappa+1}\|\bar u^\varepsilon_f\|^2_{\Gamma^T} + \varepsilon^{\lambda+1}\|\partial_y\bar u^\varepsilon_f\|^2_{\Gamma^T} + \|\bar u^\varepsilon_f\|_{L^\infty(\Gamma^T)} + \varepsilon^{\kappa+1}\|\breve u^\varepsilon_f\|^2_{(0,T)} + \|\breve u^\varepsilon_f\|_{L^\infty(0,T)} \leq C. \tag{71}$$

For $\kappa = -1$ and $\lambda \leq -1$, the effective model contains the time derivative of the fracture saturation. We proceed as for Lemma 17, but now for the Kirchhoff transformed and rescaled weak formulation of the time-discrete problem $\mathcal{P}_\Omega$ in Definition 8. We

729 introduce

(72)

$$A^\varepsilon := \begin{pmatrix} \varepsilon^{\lambda-1} & 0 \\ 0 & \varepsilon^{\lambda+1} \end{pmatrix}, \qquad u := \sum_{j=1}^{2} u_{m_j}\chi_{m_j} + \tilde{u}_f\chi_f,$$

730 $$f := \sum_{j=1}^{2} f_{m_j}\chi_{m_j} + \varepsilon\tilde{f}_f\chi_f, \qquad \vec{g}(u) := \sum_{j=1}^{2} \nabla u_{m_j}\chi_{m_j} + A^\varepsilon\nabla\tilde{u}_f\chi_f,$$

$$b(u) := \sum_{j=1}^{2} b_m(u_{m_j})\chi_{m_j} + \varepsilon^{\kappa+1} b_f(\tilde{u}_f)\chi_f,$$

731 and define $\hat{b}_{\Delta t}$ as the piecewise linear interpolation of b, in analogy to $\hat{S}_{\Delta t}$ in (23).
732 With $\Omega = \Omega_{m_1} \cup \Omega_{m_2} \cup \Omega_f^1 \cup \Gamma_1 \cup \Gamma_2$ we obtain (see (66) for the powers of ε)

733 (73)

$$\begin{aligned} \left|\langle \partial_t \hat{b}_{\Delta t}(t), \phi\rangle_{W^{-1,2}(\Omega), W_0^{1,2}(\Omega)}\right| &= \left| \left(\frac{b(u^k) - b(u^{k-1})}{\Delta t}, \phi\right)_\Omega \right| \\ &\le \left| \left(\vec{g}(u^k), \nabla\phi\right)_\Omega \right| + \left| \left(f^k, \phi\right)_\Omega \right| \\ &\le \|\phi\|_{W^{1,2}(\Omega)} \left(\sum_{j=1}^{2} \|\nabla u_{m_j}^k\|_{\Omega_{m_j}} + \|A^\varepsilon \nabla \tilde{u}_f^k\|_{\Omega_f^1} \right. \\ &\qquad \left. + \sum_{j=1}^{2} \|f_{m_j}^k\|_{\Omega_{m_j}} + \varepsilon \|\tilde{f}_f^k\|_{\Omega_f^1} \right). \end{aligned}$$

734 For $\lambda \le -1$ and $\kappa \ge -1$, a discrete form of Lemma 23 yields uniform bounds for the
735 right hand side from which we obtain after integrating in time

$$\|\partial_t \hat{b}_{\Delta t}\|_{L^2(0,T;W^{-1,2}(\Omega))} \le C,$$

737 with C independent of ε.
738 Recalling that $b(u) := \sum_{j=1}^{2} b_m(u_{m_j})\chi_{m_j} + \varepsilon^{\kappa+1} b_f(\tilde{u}_f)\chi_f$, we derive as in Lemma 17
739 for $\hat{S}_{\Delta t}^f$ that

$$\|\partial_t \hat{b}_{\Delta t}^f\|_{L^2(0,T;W^{-1,2}(\Omega_f^1))} \le C\varepsilon^{-\kappa-1},$$

741 which is uniformly bounded in ε for $\kappa \le -1$. This proves

742 LEMMA 25. *The functional $\partial_t b_f$ is uniformly bounded w.r.t. ε in $L^2(0,T;W^{-1,2}(\Omega_f^1))$*
743 *for $\kappa = -1$, $\lambda \le -1$.*

744 To obtain ε independent estimates, assumptions for the initial saturation and the
745 source term in the fracture are needed. More precisely, if $\kappa > 0$, this means that
746 the source in the fracture must approach 0 when $\varepsilon \to 0$. This is natural since for
747 $\kappa > 0$, the fracture porosity becomes smaller as the ratio of fracture width and length
748 vanishes. In this case the fracture does not have enough capacity to store water, so
749 having large source or sink terms would lead to an unphysical flow regime.
750 Also, if $\lambda < 0$, the gradient of the initial pressure in the fracture is required to
751 converge to zero rapidly enough. This can be understood as follows: for negative λ, the
752 fracture is highly conductive as compared to the solid matrix blocks and in the limit of

vanishing fracture width, the fracture becomes so permeable that pressure differences are quickly equilibrated within the fracture (even instantaneously for $\lambda < -1$, so, the solution of the effective model is spatially constant). This behaviour must be accounted for by the initial pressure gradient in the fracture.

By compactness arguments, the estimates above provide the following convergence along a sequence $\varepsilon \to 0$

$$\begin{aligned} u^\varepsilon_{m_j} &\to U_{m_j} && \text{strongly in } L^2(0,T;L^2(\Omega_{m_j})),\\ u^\varepsilon_{m_j} &\rightharpoonup U_{m_j} && \text{weakly in } L^2(0,T;\mathcal{V}_{m_j}),\\ \bar{u}^\varepsilon_f &\rightharpoonup \bar{U}_f && \text{weakly in } L^2(0,T;L^2(\Gamma)). \end{aligned} \tag{74}$$

For $\lambda \le -1$, the gradient of the fracture solution $\nabla \tilde{u}^\varepsilon_f$ is bounded in $L^2(0,T;L^2(\Omega_f))$ according to Lemma 23. From this, we infer just as for the matrix block solutions in equation (74) that there exists a subsequence of $\varepsilon \to 0$ along which

$$\begin{aligned} \tilde{u}^\varepsilon_f &\to U_f, && \text{strongly in } L^2(0,T;L^2(\Omega_f)),\\ \bar{u}^\varepsilon_f &\to \bar{U}_f, && \text{strongly in } L^2(0,T;L^2(\Gamma)),\\ \bar{u}^\varepsilon_f &\rightharpoonup \bar{U}_f && \text{weakly in } L^2(0,T;\bar{\mathcal{V}}_f),\\ \breve{u}^\varepsilon_f &\to \breve{U}_f && \text{strongly in } L^2(0,T). \end{aligned} \tag{75}$$

The following result, nothing but Proposition 4.3 in [20] will also be used for deriving the effective model in the fracture

PROPOSITION 26. *Let $\Omega = (-\frac{1}{2},\frac{1}{2}) \times (0,L)$, $f \in W^{1,2}(\Omega)$, and let $\bar{f} : [0,L] \to \mathbb{R}$ be defined as $\bar{f}(y) = \int_{-\frac{1}{2}}^{\frac{1}{2}} f(\xi,y)\, d\xi$. Then, in the sense of traces*

$$\|f(\xi_0,\cdot) - \bar{f}\|_{(0,L)} \le \|\partial_\xi f\|_\Omega, \tag{76}$$

for each $\xi_0 \in [-\frac{1}{2},\frac{1}{2}]$.

This proposition and Lemma 23 yield the following estimate:

LEMMA 27. *There exists a $C > 0$ independent of ε such that for any $z_0 \in [-\frac{1}{2},\frac{1}{2}]$ it holds*

$$\|\tilde{u}^\varepsilon_f(\cdot,z_0,\cdot) - \bar{u}^\varepsilon_f\|_{\Gamma^T} \le \varepsilon^{\frac{1-\lambda}{2}} C. \tag{77}$$

Lemma 27 shows that $\lambda = 1$ ensures that the L^2 distance between the Kirchhoff transformed pressure and its z-average remains bounded as $\varepsilon \to 0$, while $\lambda < 1$ provides the convergence.

5.3. Upscaling results. It remains to show that the limit functions are a solution to the respective effective model. We have

THEOREM 28 (Upscaling theorem). *Depending on the range of κ and λ, the limit 3-tupels are weak solutions to the effective models listed below:*

$$\begin{aligned} &\kappa = -1, && \lambda = -1 : && (U_{m_1}, U_{m_2}, \bar{U}_f) && \text{Effective model I},\\ &\kappa \in (-1,\infty), && \lambda = -1 : && (U_{m_1}, U_{m_2}, \bar{U}_f) && \text{Effective model II},\\ &\kappa = -1, && \lambda \in (-\infty,-1) : && (U_{m_1}, U_{m_2}, \breve{U}_f) && \text{Effective model III},\\ &\kappa \in (-1,\infty), && \lambda \in (-\infty,-1) : && (U_{m_1}, U_{m_2}, \breve{U}_f) && \text{Effective model IV},\\ &\kappa \in (-1,\infty), && \lambda \in (-1,1) : && (U_{m_1}, U_{m_2}, \bar{U}_f) && \text{Effective model V}. \end{aligned} \tag{78}$$

Proof. We give the proof for $\lambda \geq -1$. The cases $\lambda < -1$ are analogous, but require using spatially constant test functions for the fracture equation (69), i.e. $\phi_f(t,z,y) = \phi_f(t)$. Note that for homogeneous Dirichlet boundary conditions, the fracture equations in Effective models III and IV reduce to $\psi_f \equiv 0$ (see Remark 2).

We test with $(\phi_{m_1}, \phi_{m_2}, \phi_f) \in W^{1,2}(0,T;\mathcal{V}_{m_1}) \times W^{1,2}(0,T;\mathcal{V}_{m_2}) \times W^{1,2}(0,T;\bar{\mathcal{V}}_f)$ satisfying $\phi_{m_1}(t,z,y)|_{\Gamma_1} = \phi_f(t,y) = \phi_{m_2}(t,z,y)|_{\Gamma_2}$ for a.e. $t \in [0,T]$ and $\phi_\rho(T) = 0$ for $\rho \in \{m_1, m_2, f\}$ and denote the terms in (69) by $I_1, \dots, I_8$. For all values of κ and λ, the term I_6 vanishes in the limit $\varepsilon \to 0$ as

$$|I_6| = \varepsilon \left| \left(\bar{f}_f^\varepsilon, \phi_f\right)_{\Gamma^T} \right| \leq \varepsilon \|\bar{f}_f^\varepsilon\|_{\Gamma^T} \|\phi_f\|_{\Gamma^T} \to 0.$$

The terms I_5 and I_7 do not depend on ε and remain unchanged as ε approaches zero. The strong L^2 convergence in $(74)_1$ and the Lipschitz continuity of b_m give

$$I_1 = -\sum_{j=1}^{2} \left(b_m(u_{m_j}^\varepsilon), \partial_t \phi_{m_j}\right)_{\Omega_{m_j}^T} \to -\sum_{j=1}^{2} \left(b_m(U_{m_j}), \partial_t \phi_{m_j}\right)_{\Omega_{m_j}^T}.$$

The weak convergence in $(74)_2$ yields

$$I_3 = \sum_{j=1}^{2} \left(\nabla u_{m_j}^\varepsilon, \nabla \phi_{m_j}\right)_{\Omega_{m_j}^T} \to \sum_{j=1}^{2} \left(\nabla U_{m_j}, \nabla \phi_{m_j}\right)_{\Omega_{m_j}^T}.$$

As regards the fracture solution, we distinguish the cases $\lambda = -1$ and $\lambda > -1$: in case of $\lambda = -1$, the weak convergence in $(75)_3$ leads to

$$I_4 = \left(\partial_y \bar{u}_f^\varepsilon, \partial_y \phi_f\right)_{\Gamma^T} \to \left(\partial_y \bar{U}_f, \partial_y \phi_f\right)_{\Gamma^T},$$

whereas for $\lambda > -1$, we get

$$|I_4| = \varepsilon^{\lambda+1} \left| \left(\partial_y \bar{u}_f^\varepsilon, \partial_y \phi_f\right)_{\Gamma^T} \right| \leq \varepsilon^{\lambda+1} \|\partial_y \bar{u}_f^\varepsilon\|_{\Gamma^T} \|\partial_y \phi_f\|_{\Gamma^T} \leq \varepsilon^{\frac{\lambda+1}{2}} C \|\partial_y \phi_f\|_{\Gamma^T} \to 0,$$

where we made use of the estimate for $\partial_y \bar{u}_f^\varepsilon$ in Lemma 24.

It remains to consider the terms I_2 and I_8. Here, we make a distinction between the cases $\kappa = -1$ and $\kappa > -1$. First, consider the case $\kappa = -1$, where $I_2 = -\left(\bar{b}_f(\tilde{u}_f^\varepsilon), \partial_t \phi_f\right)_{\Gamma^T}$ and I_8 is independent of ε.
For the term I_2, we start by estimating

$$\begin{aligned} \left| \left(\bar{b}_f(\tilde{u}_f^\varepsilon) - b_f(\bar{U}_f), \partial_t \phi_f\right)_{\Gamma^T} \right| \leq & \left| \left(\bar{b}_f(\tilde{u}_f^\varepsilon) - b_f(\bar{u}_f^\varepsilon), \partial_t \phi_f\right)_{\Gamma^T} \right| \\ & + \left| \left(b_f(\bar{u}_f^\varepsilon) - b_f(\bar{U}_f), \partial_t \phi_f\right)_{\Gamma^T} \right|. \end{aligned}$$

For the first term on the right hand side we obtain using the Lipschitz continuity of

b_f and Lemma 27

$$\begin{aligned}\left|\left(\bar{b}_f(\tilde{u}_f^\varepsilon)-b_f(\bar{u}_f^\varepsilon),\partial_t\phi_f\right)_{\Gamma^T}\right| &\le \left\|\int_{-\frac{1}{2}}^{\frac{1}{2}}\left(b_f(\tilde{u}_f^\varepsilon)-b_f(\bar{u}_f^\varepsilon)\right)dz\right\|_{\Gamma^T}\|\partial_t\phi_f\|_{\Gamma^T}\\ &\le M_S\left\|\int_{-\frac{1}{2}}^{\frac{1}{2}}\left|\tilde{u}_f^\varepsilon-\bar{u}_f^\varepsilon\right|dz\right\|_{\Gamma^T}\|\partial_t\phi_f\|_{\Gamma^T}\\ &\le M_S C\,\varepsilon^{\frac{1-\lambda}{2}}\|\partial_t\phi_f\|_{\Gamma^T},\end{aligned}$$

which approaches zero as $\varepsilon\to 0$.
Due to the strong convergence in $(75)_2$, the second term vanishes:

$$\left|\left(b_f(\bar{u}_f^\varepsilon)-b_f(\bar{U}_f),\partial_t\phi_f\right)_{\Gamma^T}\right| \le M_S\|\bar{u}_f^\varepsilon-\bar{U}_f\|_{\Gamma^T}\|\partial_t\phi_f\|_{\Gamma^T}.$$

This shows that

$$I_2=-\left(\bar{b}_f(\tilde{u}_f^\varepsilon),\partial_t\phi_f\right)_{\Gamma^T}\to-\left(b_f(\bar{U}_f),\partial_t\phi_f\right)_{\Gamma^T}.$$

For $\kappa>-1$, we estimate

$$|I_2|=\varepsilon^{\kappa+1}\left|\left(\bar{b}_f(\tilde{u}_f^\varepsilon),\partial_t\phi_f\right)_{\Gamma^T}\right|\le\varepsilon^{\kappa+1}M_S\|\tilde{u}_f^\varepsilon\|_{\Omega_f^T}\|\partial_t\phi_f\|_{\Gamma^T}\le\varepsilon^{\frac{\kappa+1}{2}}M_SC\|\partial_t\phi_f\|_{\Gamma^T},$$

which vanishes in view of Lemma 24. Similarly,

$$|I_8|=\varepsilon^{\kappa+1}\left|\left(\bar{b}_f(\tilde{u}_{f,I}),\phi_f(0)\right)_{\Gamma}\right|\le\varepsilon^{\kappa+1}M_S\|\tilde{u}_{f,I}\|_{\Omega_f}\|\phi_f(0)\|_{\Gamma}\le\varepsilon^{\frac{\kappa+1}{2}}M_SC\|\phi_f(0)\|_{\Gamma}$$

vanishes in the limit.

Finally, the Dirichlet interface condition for the pressure head has to be proven. It turns out that a weakly convergent subsequence in $L^2(0,T;L^2(\Gamma))$ in the fracture suffices for this purpose. As the weak convergence of $\bar{u}_f^\varepsilon$ towards $\bar{U}_f$ does not directly imply the weak convergence of $\mathcal{K}_f^{-1}(\bar{u}_f^\varepsilon)$ towards $\mathcal{K}_f^{-1}(\bar{U}_f)$, we define the function $\mathcal{R}(u_{m_j}):=(\mathcal{K}_f\circ\mathcal{K}_m^{-1})(u_{m_j})$ in order to transform the interface condition $\mathcal{K}_m^{-1}(U_{m_j})=\mathcal{K}_f^{-1}(\bar{U}_f)$ on Γ_j into a linear expression in $\bar{U}_f$, namely

$$\mathcal{R}(U_{m_j})=\bar{U}_f\qquad\text{on }\Gamma_j.$$

Now we take an arbitrary test function $\phi\in L^2(0,T;L^2(\Gamma_j))$ and estimate

$$\begin{aligned}\left|\left(\mathcal{R}(U_{m_j})-\bar{U}_f,\phi\right)_{\Gamma_j^T}\right| &\le \left|\left(\mathcal{R}(U_{m_j})-\mathcal{R}(u_{m_j}^\varepsilon),\phi\right)_{\Gamma_j^T}\right|+\left|\left(\mathcal{R}(u_{m_j}^\varepsilon)-\tilde{u}_f^\varepsilon,\phi\right)_{\Gamma_j^T}\right|\\ &\quad+\left|\left(\tilde{u}_f^\varepsilon-\bar{u}_f^\varepsilon,\phi\right)_{\Gamma_j^T}\right|+\left|\left(\bar{u}_f^\varepsilon-\bar{U}_f,\phi\right)_{\Gamma_j^T}\right|.\end{aligned}$$

Let us denote the terms on the right hand side by $J_1,\dots,J_4$. As $u_{m_j}^\varepsilon$ and $\tilde{u}_f^\varepsilon$ satisfy the interface condition, we immediately get $J_2=0$. Note that Assumption (A_K) implies the Lipschitz continuity of $\mathcal{R}$ with Lipschitz constant $\frac{M_K}{m_K}$. Making use of this and the Cauchy–Schwarz inequality yields

$$J_1\le\frac{M_K}{m_K}\|U_{m_j}-u_{m_j}^\varepsilon\|_{\Gamma_j^T}\|\phi\|_{\Gamma_j^T},$$

and one shows as in the proof of Theorem 20 that $J_1 \to 0$ in the limit $\varepsilon \to 0$ using the trace inequality, the strong convergence in equation $(74)_1$ and the boundedness of the gradient due to the weak convergence in equation $(74)_2$. For the term J_3, we obtain

$$J_3 \leq \|\tilde{u}_f^\varepsilon - \bar{u}_f^\varepsilon\|_{\Gamma_j^T} \|\phi\|_{\Gamma_j^T},$$

and from Lemma 27 we infer that $J_3 \to 0$. Finally, the weak convergence in equation $(75)_3$ yields $J_4 \to 0$. Since $\phi \in L^2(0,T;L^2(\Gamma_j))$ was arbitrary, one has $\mathcal{R}(U_{m_j}) = \bar{U}_f$ on Γ_j and therefore $\mathcal{K}_m^{-1}(U_{m_j}) = \mathcal{K}_f^{-1}(\bar{U}_f)$ on Γ_j in the sense of traces, which concludes the proof.

Remark 29. The porous matrix domain Ω_{m_1} has the interface at $x = 0$ with a fracture domain boundary that corresponds to $z = -1$ from the fracture domain side. Similarly, Ω_{m_2} has the interface at $x = 0$ with fracture domain boundary at $z = 1$. The two interfaces become one in the reduced dimensional model, and the solution in the fracture domain is independent of z (see the effective models I – V above). Therefore the fracture model component becomes an effective boundary condition for the two model components defined in the porous matrices.

Remark 30. We remark now the reason for leaving out the case when $\kappa = -1, \lambda \in (-1,1)$ in our analysis. From (74) we get the boundedness of u_f^ε and the smoothness of $\bar{b}_f(u_f^\varepsilon)$ implies the existence of a weak limit for $\bar{b}_f^\varepsilon$. However, the identification of this limit in (69) to $\bar{b}_f(u_f)$ requires a strong convergence of $\bar{u}_f^\varepsilon$. However, Lemma 24 does not give an estimate for $\nabla \bar{u}_f^\varepsilon$ that is uniform with respect to ε. Therefore, the strong convergence of $\bar{u}_f^\varepsilon$ cannot be deduced. This is why the case mentioned above is not taken in the present analysis.

6. Numerical simulations. This section presents some numerical examples to validate the theoretical upscaling results. The simulations are carried out using a standard finite volume scheme implemented in MATLAB. We use a matching grid, composed of uniform rectangular cells for partitioning the two-dimensional subdomains, and intervals of equal size for the one-dimensional fracture in the effective models. The flux is computed with a two-point flux approximation (TPFA) scheme. We use an implicit Euler discretisation in time with fixed time step, and the modified Picard scheme for the linearisation. We adopt a monolithic approach and solve the system of equations for the entire domain at once.

The numerical example models the injection of water into an aquifer which is crossed by a fracture. The boundary and initial conditions are illustrated in Figure 3. Although the analysis is given for homogeneous Dirichlet conditions, we expect the theoretical results to hold for more general boundary conditions, as considered in the numerical example. In the simulations with a two-dimensional fracture, the dimensionless fracture width takes the values $\varepsilon \in \{10^{-k} : k \in \{0,1,2,3,4\}\}$. We impose no flow boundary conditions excepting the inflow region on the central lower edge of the left matrix block subdomain, namely for $(x,y) \in [-1-\frac{\varepsilon}{2}+\frac{1}{4}, -\frac{\varepsilon}{2}-\frac{1}{4}]\times\{0\}$, and the right upper boundary, for $(x,y) \in [\frac{\varepsilon}{2}+\frac{1}{4}, 1+\frac{\varepsilon}{2}-\frac{1}{4}]\times\{1\}$, where a Dirichlet condition allows for outflow. Thus, the water must cross the fracture to leave the domain. The van Genuchten parametrisation (see [29]) of the $S-\psi$, respectively $K-S$ relationships are given in Figure 3. These parameters correspond to silt loam in the matrix, respectively the Touchet silt loam in the fracture. As the fracture width goes to zero, the storage term and the flux term in the fracture are scaled with

ε^κ and ε^λ, respectively (see Problem $\mathcal{P}_\varepsilon$) in order to investigate the convergence of the full models towards the effective models. We refer to [41] for more numerical examples discussing how well the effective models approximate the full models for certain choices of fixed soil properties and fracture widths.

We take the end time of the simulation to be $T = 0.75$. The time step is chosen as 0.005. The grid size is taken as $\Delta x = \Delta y = 1/160$ in the matrix blocks and $\Delta y = 1/160$ and $\Delta x \in \{1/160, 1/800, 1/4000, 1/20000, 1/100000\}$ in the fracture, corresponding to the different fracture widths ε. This means that the thinnest two-dimensional fracture with $\varepsilon = 10^{-4}$ has a thickness of 10 cells in x-direction.

Geometry

$\Omega_{m_1} = (-1-\varepsilon/2, -\varepsilon/2) \times (0,1)$
$\Omega_{m_2} = (\varepsilon/2, 1+\varepsilon/2) \times (0,1)$
$\Omega_f^\varepsilon = (-\varepsilon/2, \varepsilon/2) \times (0,1)$

Initial condition and source term

$\psi_I \equiv -3$
$f \equiv 0$

Van Genuchten parameters

	Fracture	Solid matrix
α	0.500	0.423
θ_S	0.469	0.396
θ_R	0.190	0.131
n	7.09	2.06
$K_{S,f}/K_{S,m}$	61.09	

Boundary conditions

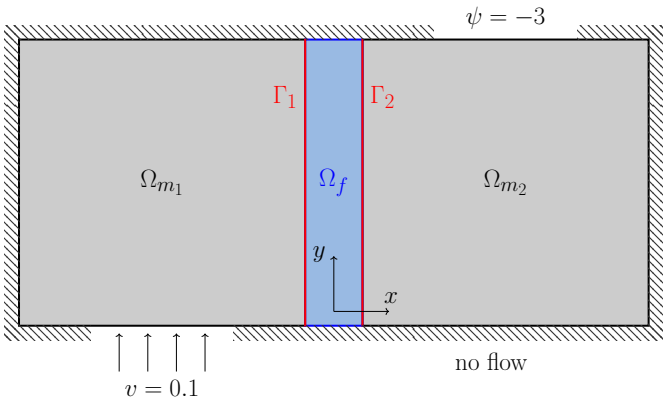

FIG. 3. *Simulation parameters for the realistic example: geometry, initial and boundary conditions, and van Genuchten parameters*

In dimensionless setting, the van Genuchten–Mualem parametrisation becomes (see also Figure 4)

$$S_\rho(\psi_\rho) = \begin{cases} \frac{\theta_{R,\rho}}{\theta_{S,\rho}} + (1 - \frac{\theta_{R,\rho}}{\theta_{S,\rho}}) \left[\frac{1}{1+(-\alpha_\rho \psi_\rho)^{n_\rho}}\right]^{\frac{n_\rho - 1}{n_\rho}}, & \psi_\rho \le 0, \\ \theta_{S,\rho}, & \psi_\rho > 0, \end{cases}$$

$$K_\rho(S_\rho(\psi_\rho)) = \begin{cases} \Theta_{\text{eff},\rho}(\psi_\rho)^{\frac{1}{2}} \left[1 - \left(1 - \Theta_{\text{eff},\rho}(\psi_\rho)^{\frac{n_\rho}{n_\rho - 1}}\right)^{\frac{n_\rho - 1}{n_\rho}}\right]^2, & \psi_\rho \le 0, \\ 1, & \psi_\rho > 0, \end{cases} \tag{79}$$

where θ_S stands for the water content of the fully saturated porous medium, θ_R denotes the residual water content, α and n are curve fitting parameters expressing

the soil properties, and $\Theta_{\text{eff}}(\psi) := \frac{\theta(\psi)-\theta_R}{\theta_S-\theta_R}$ is the effective saturation.

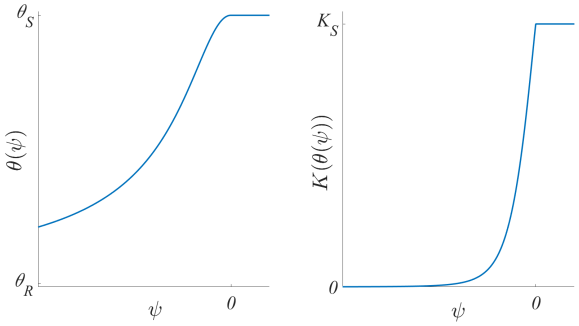

FIG. 4. *Schematic plot of the hydraulic relationships $\theta(\psi)$ and $K(\theta(\psi))$ in the van Genuchten–Mualem model*

The ratio of the porosities, respectively of the absolute hydraulic conductivities are given by

$$\frac{\phi_f}{\phi_m} = \frac{\theta_{S,f}}{\theta_{S,m}}\varepsilon^{\kappa}, \qquad \text{and} \qquad \frac{\bar{K}_{a,f}}{\bar{K}_{a,m}} = \frac{K_{S,f}}{K_{S,m}}\varepsilon^{\lambda}, \tag{80}$$

respectively, where K_S denotes the saturated hydraulic conductivity.
We consider two choices for κ and λ in this example:

a) $\kappa = \lambda = -1$,
b) $\kappa = \lambda = 0$.

In the limit $\varepsilon \to 0$, we expect the solution to converge towards Effective model I with the one-dimensional Richards equation governing the flow in the fracture in case a), while theory predicts convergence towards Effective model V in case b), where pressure and flux are continuous across the interface.

Figure 5 depicts the pressure head of the effective models at final time $t = T$. In the subdomain Ω_{m_1} the pressure has risen due to the injection of water from the boundary. While the solutions in the two effective models look similar at first glance, notice the kink in Effective model I at the fracture which reflects the difference in the normal fluxes obtained in the matrix domains at the reduced-dimensional fracture. this difference is due to the storage of water in the fracture. In contrast, the fracture has disappeared in Effective model V causing the pressure to be smooth. Besides, the storage term in Effective model I slows down the propagation of water into subdomain Ω_{m_2}, which is reflected in the lower pressure on the right of the fracture as compared to Effective model V.

Figures 6 and 7 show the x-averaged pressure head in the fracture for the full models and the corresponding effective model for case a) and b), respectively. Below, the difference $\bar{\psi} - \psi_{\text{eff}}$ between each model and the effective model is depicted in a symmetric logarithmic scale (see [68]).

In both cases, the convergence towards the respective effective model is evident. In case a), the difference between the full model with $\varepsilon = 10^{-1}$ and Effective model I is smaller than 10^{-3} at each y-position and decreases further as the fracture becomes thinner. For $\varepsilon = 10^{-3}$, the difference amounts to less than 10^{-7} and does not improve much further for $\varepsilon = 10^{-4}$ since we are well below the tolerance of the nonlinear

solver, which is set here to 10^{-5}. For ε between 1 and 10^{-3}, the averaged pressure in the full models is higher than in the effective model along the entire fracture and decreases monotonically as ε goes to zero.

In case b), we observe slower convergence towards Effective model V. This is in line with the estimate in Lemma 27 that provides for faster convergence for smaller values of λ. Nonetheless, for $\varepsilon = 1$, the difference between the full model and the effective model is greater than 0.1 and drops to less than 2×10^{-4} for $\varepsilon = 10^{-4}$.

In order to quantify the convergence speed for both case, we plot the error in pressure head towards the respective effective model in Figure 8, split up into the fracture and the solid matrix blocks. The grey triangles indicate convergence rates of one and two, respectively. The convergence is faster in case a) than in case b), which is expected in view of the estimate in (77) due to the sharper bound for the derivative of the pressure perpendicular to the fracture. For case a), quadratic convergence is achieved until well below the tolerance of the nonlinear solver. In case b), we obtain linear convergence and for $\varepsilon = 10^{-4}$, the L^2-error amounts to less than 10^{-4} in all subdomains.

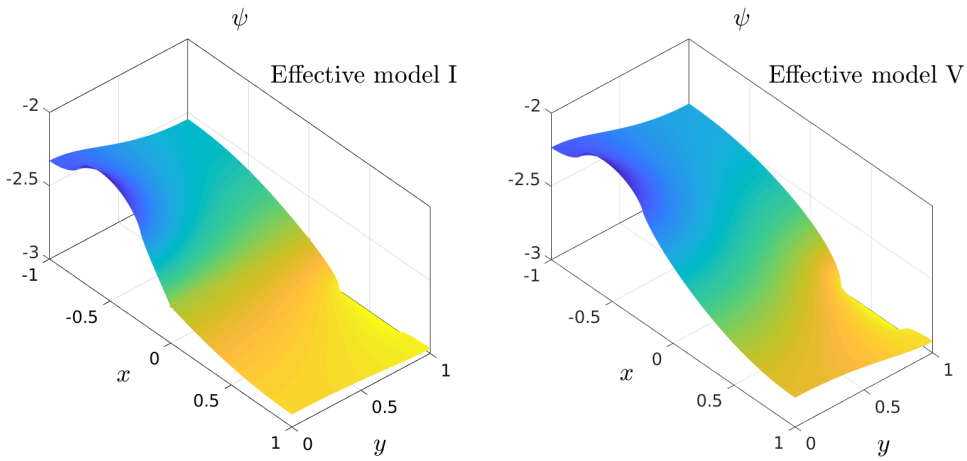

FIG. 5. *Solution to the effective models at $t = 0.75$: pressure head ψ of Effective model I (left) and Effective model V (right).*

7. Conclusion. We have developed effective equations for unsaturated flow in a two-dimensional porous medium consisting of two porous blocks separated by a thin, porous fracture. The flow is modeled by the Richards equation in both blocks, as well as in the fracture. The fracture shape is characterized by ε, a small parameter expressing the ratio of the fracture wdth and its length. The effective models are derived rigorously in the limit case when $\varepsilon \to 0$, so the fracture is reduced to a one-dimensional object which becomes an interface between the adjacent blocks. Whereas the effective model in the porous blocks remains the Richards equation, the one in the reduced-dimensional fracture depends on two additional parameters, κ and λ. These describe how the ratios of the porosities, respectively of the absolute permeabilities in the two different types of media (the fracture and the porous blocks) depend on ε, namely ε^κ and ε^λ. Different regimes are considered, covering the cases $\kappa > -1, \lambda < 1$, corresponding to situations in which, compared to the porous blocks, the fracture is highly or less permeable, and has a high capacity to store fluid or not. The rigorous convergence proofs given here are sustained by preliminary numerical examples.

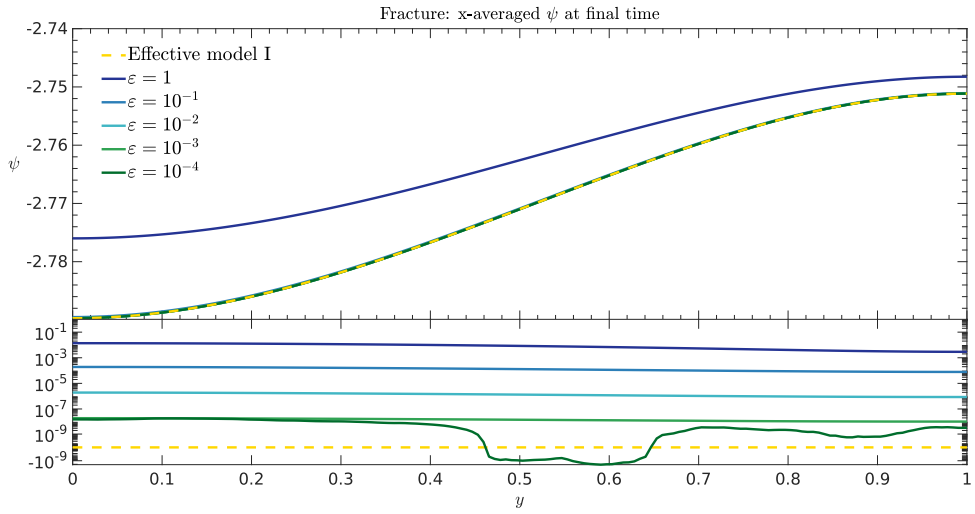

FIG. 6. *Case a): x-averaged fracture solution along the fracture for different ε and for Effective model I at $t = T$. The error with respect to the effective model is shown below.*

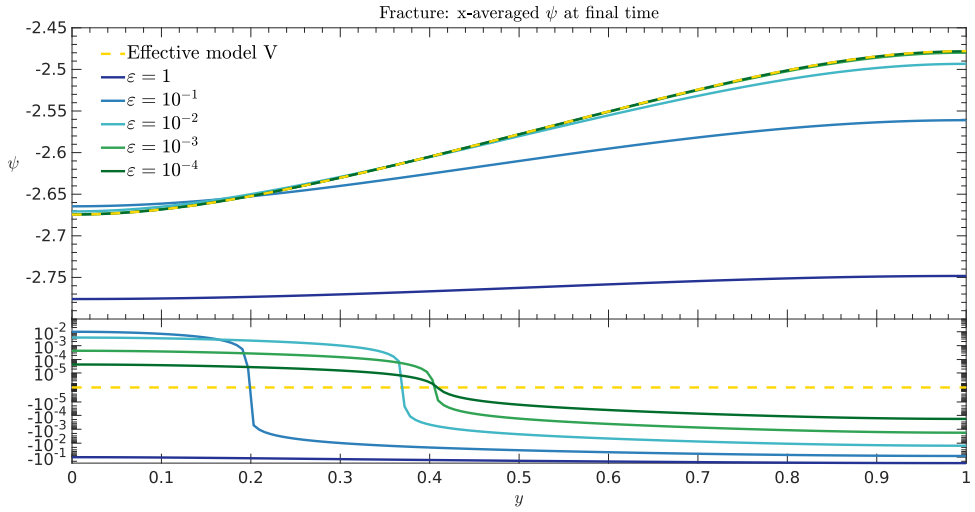

FIG. 7. *Case b): x-averaged fracture solution along the fracture for different ε and for Effective model V at $t = T$. The error with respect to the effective model is shown below.*

8. Acknowledgements. The authors would like to thank Dr. Markus Gahn for the fruitful discussions and valuable suggestions. The work of K. Kumar and F.A. Radu was partially supported by the Research Council of Norway through the projects Lab2Field no. 811716, IMMENS no. 255426, CHI no. 25510 and Norwegian Academy of Science and Statoil through VISTA AdaSim no. 6367. I.S. Pop was supported by the Research Foundation-Flanders (FWO) through the Odysseus programme (project GOG1316N) and by Statoil through the Akademia agreement.

REFERENCES

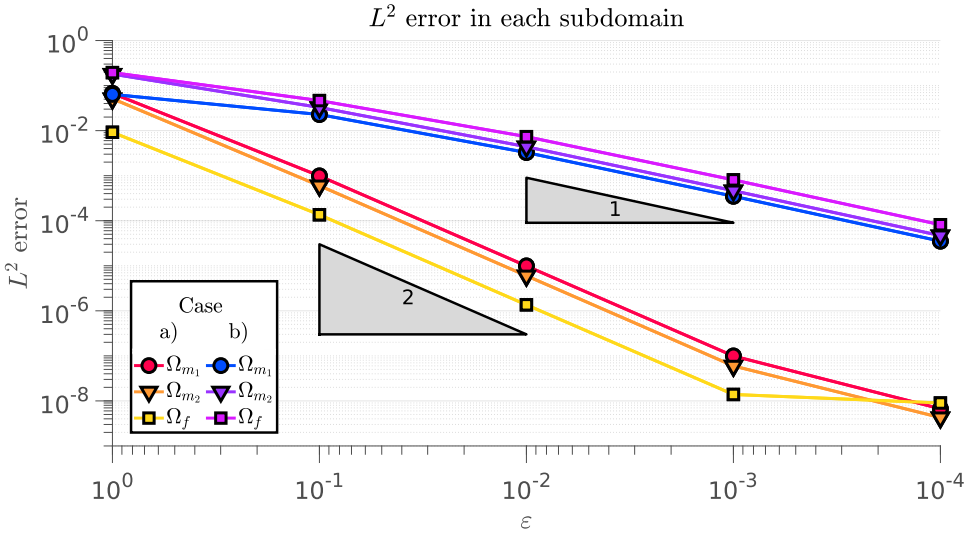

FIG. 8. *L^2 error with respect to the corresponding effective model in each subdomain for both cases. In the fracture domain Ω_f, the error is between the x-averaged pressure head and the one-dimensional pressure head of the effective model. The grey triangles indicate convergence rates of 1 and 2, respectively.*

[1] P. ADLER AND J. THOVERT, *Fractures and Fracture Networks*, Theory and Applications of Transport in Porous Media, Springer, 1999.

[2] J. AGHILI, K. BRENNER, J. HENNICKER, R. MASSON AND L. TRENTY, *Two-phase Discrete Fracture Matrix models with linear and nonlinear transmission conditions*, GEM Int. J. Geomath. 10: 1, (2019).

[3] E. AHMED, J. JAFFRÉ AND J.E. ROBERTS, *A reduced fracture model for two-phase flow with different rock types*, Math. Comput. Simul., 137 (2017), pp. 49–70.

[4] H. ALT AND S. LUCKHAUS, *Quasilinear elliptic-parabolic differential equations*, Math. Z., 183 (1983), pp. 311–341.

[5] H. ALT, S. LUCKHAUS AND A. VISINTIN, *On nonstationary flow through porous media*, Ann. Mat. Pura Appl., 136 (1984), pp. 303–316.

[6] P. Ø. ANDERSEN AND S. EVJE, *A model for reactive flow in fractured porous media*, Chem. Eng. Sci., 145 (2016), pp. 196–213.

[7] P. ANGOT, F. BOYER AND F. HUBERT, *Asymptotic and numerical modelling of flows in fractured porous media*, ESAIM Math. Model. Numer. Anal., 43 (2009), pp. 239–275.

[8] T. ARBOGAST, M.F. WHEELER AND N.Y. ZHANG, *A non-linear mixed finite element method for a degenerate parabolic equation arising in flow in porous media*, SIAM J. Numer. Anal., 33 (1996), pp. 1669–1687.

[9] J.-P. AUBIN, *Un théorème de compacité*, C. R. Acad. Sci. Paris, 256 (1963), pp. 5042–5044.

[10] A. BENSOUSSAN, L. BOCCARDO AND F. MURAT, *On a non linear partial differential equation having natural growth terms and unbounded solution*, Ann. Inst. Henri Poincaré, 5 (1988), pp. 347–364.

[11] H. BERNINGER, R. KORNHUBER AND O. SANDER, *A multidomain discretization of the Richards equation in layered soil*, Comput. Geosci., 19 (2015), pp. 213–232.

[12] K. BRENNER, J. HENNICKER, R. MASSON AND P. SAMIER, *Hybrid-dimensional modelling of two-phase flow through fractured porous media with enhanced matrix fracture transmission conditions*, J. Comput. Phys., 357 (2018), pp. 100–124.

[13] L. BOCCARDO, F. MURAT AND J.P. PUEL, *Existence of bounded solutions for non linear elliptic unilateral problems*, Ann. Mat. Pura Appl., 152 (1988), pp. 183–196.

[14] W.M. BOON, J.M. NORDBOTTEN AND I. YOTOV, *Robust discretization of flow in fractured porous media*, SIAM J. Numer. Anal., 56 (2018), pp. 2203—2233.

[15] R.H. BROOKS AND A.T. COREY, *Hydraulic properties of porous media*, Hydrol. Pap. 3 (1964).

[16] M. BUKAC, I. YOTOV AND P. ZUNINO, *Dimensional model reduction for flow through fractures in poroelastic media*, ESAIM Math. Model. Numer. Anal., 51 (2017), pp. 1429–1471.

[17] C. Cancès and M. Pierre, *An existence result for multidimensional immiscible two-phase flows with discontinuous capillary pressure field*, SIAM J. Math. Anal., 44 (2012), pp. 966–992.
[18] C.J. van Duijn, J. Molenaar and M.J. de Neef, *The effect of capillary forces on immiscible two-phase flow in heterogeneous porous media*, Transp. Porous Media, 21 (1995), pp. 71–93.
[19] C.J. van Duijn and L.A. Peletier, *Nonstationary filtration in partially saturated porous media*, Arch. Rational Mech. Anal., 78 (1982), pp. 173–198.
[20] C.J. van Duijn and I.S. Pop, *Crystal dissolution and precipitation in porous media: pore scale analysis*, J. Reine. Angew. Math., 577 (2004), pp. 171–211.
[21] C.J. van Duijn, A. Mikelic and I.S. Pop, *Effective equations for two-phase flow with trapping on the micro scale*, SIAM J. Appl. Math., 62 (2002), pp. 1531–1568.
[22] C. Ebmeyer, *Error estimates for a class of degenerate parabolic equations*, SIAM J. Numer. Anal., 35 (1998), pp. 1095–1112.
[23] R. Eymard, M. Gutnic and D. Hilhorst, *The finite volume method for Richards equation*, Comput. Geosci., 3 (1999), pp. 259–294.
[24] R. Eymard, D. Hilhorst and M. Vohralík, *A combined finite volume-nonconforming/mixed-hybrid finite element scheme for degenerate parabolic problems*, Numer. Math. 105 (2006), pp. 73–131.
[25] R. Eymard, C. Guichard, R. Herbin and R. Masson, *Gradient schemes for two-phase flow in heterogeneous porous media and Richards equation*, ZAMM Z. Angew. Math. Mech., 94 (2014), pp. 560–585.
[26] A. Ferroni, L. Formaggia and A. Fumagalli, *Numerical analysis of Darcy problem on surfaces* ESAIM Math. Model. Numer. Anal., 50 (2016), pp. 1615–1630.
[27] L. Formaggia, A. Fumagalli, A. Scotti and P. Ruffo, *A reduced model for Darcy's problem in networks of fractures* ESAIM Math. Model. Numer. Anal., 48 (2014), pp. 1089–1116.
[28] T.T. Garipov, M. Karimi-Fard and H.A. Tchelepi, *Discrete fracture model for coupled flow and geomechanics*, Comput. Geosci., 20 (2016), pp. 149–10.
[29] M.Th. van Genuchten, *A closed-form equation for predicting the hydraulic conductivity of unsaturated soils*, Soil Sci. Soc. Am. J., 44 (1980), pp. 892–898.
[30] D. Gilbarg and N.S. Trudinger, *Elliptic Partial Differential Equations of Second Order*, Springer, 1998.
[31] V. Girault, K. Kumar and M.F. Wheeler, *Convergence of iterative coupling of geomechanics with flow in a fractured poroelastic medium*, Comp. Geosci., 20 (2016), pp. 997–1011.
[32] D. Gläser, R. Helmig, B. Flemisch and H. Class, *A discrete fracture model for two-phase fow in fractured porous media*, Adv. Water Resour., 110 (2017), pp. 335–348.
[33] R. Helmig, *Multiphase flow and transport processes in the subsurface: a contribution to the modeling of hydrosystems*, Springer-Verlag, 1997.
[34] P. Henning, M. Ohlberger and B. Schweizer, *Homogenization of the degenerate two-phase flow equations*, Math. Models Methods Appl. Sci. (M3AS), 23 (2013), pp. 2323–2352.
[35] E. Hough, J.M. Pearce, S.J. Kemp and G.M. Williams, *An investigation of some sediment-filled fractures within redbed sandstones of the UK*, Proceedings of the Yorkshire Geological Society, 56 (2006), pp. 41–53.
[36] W. Jäger and N. Kutev, *Discontinuous solutions of the nonlinear transmission problem for quasilinear elliptic equations*, IWR Preprint 1998–22, Universit at Heidelberg, 1998.
[37] W. Jäger and L. Simon, *On transmission problems for nonlinear parabolic differential equations*, Ann. Univ. Sci. Budapest, 45 (2002), pp. 143–168.
[38] J. Kačur, *Method of Rothe in evolution equations*, Teubner-Texte zur Mathematik Vol. 80, B.G. Teubner, Leipzig, 1985.
[39] M. Karimi-Fard, L.J. Durlofsky and K. Aziz, *An efficient discrete-fracture model applicable for general-purpose reservoir simulators*, SPE Journal, 9 (2004), pp. 227–236.
[40] R.A. Klausen, F.A. Radu and G.T. Eigestad, *Convergence of MPFA on triangulations and for Richards' equation*, Int. J. Numer. Meth. Fluids, 58 (2008), pp. 1327–1351.
[41] K. Kumar, F. List, I.S. Pop and F.A. Radu, *Formal upscaling and numerical validation of fractured flow models for Richards' equation*, CMAT Report UP-19-03, Hasselt University, 2019.
[42] M. Lenzinger and B. Schweizer, *Two-phase flow equations with outflow boundary conditions in the hydrophobic–hydrophilic case*, Nonlinear Anal., 73 (2010), pp. 840–853.
[43] F. List, *Upscaling of Richards' Equation in Fractured Porous Media*, Master Thesis, Eindhoven University of Technology, 2017.
[44] F. List and F.A. Radu, *A study on iterative methods for solving Richards' equation*, Comput. Geosci., 20 (201), pp. 341–353.
[45] M. Marcus and V.J. Mizel, *Complete characterization of functions which act, via superpo-*

sition, on Sobolev spaces, Trans. Amer. Math. Soc., 251 (1979), pp. 187–218.
[46] V. Martin, J. Jaffré and J.E. Roberts, *Modeling fractures and barriers as interfaces for flow in porous media*, SIAM J. Sci. Comp., 26 (2005), pp. 1667–1691.
[47] A. Mikelic, M.F. Wheeler and T. Wick, *A phase-field method for propagating fluid-filled fractures coupled to a surrounding porous medium*, Multiscale Model. Simul., 13 (2015), pp. 367–398.
[48] K. Mitra and I.S. Pop, *A modified L-scheme to solve nonlinear diffusion problems*, Comp. Math. Appl., 77 (2019), pp. 1722–1738.
[49] F. Morales and R.E. Showalter, *The narrow fracture approximation by channeled flow*, J. Math. Anal. Appl., 365 (2010), pp. 320–331.
[50] F. Morales and R.E. Showalter, *Interface approximation of Darcy flow in a narrow channel*, Math. Methods Appl. Sci., 35 (2012), pp. 182–195.
[51] F. Morales and R.E. Showalter, *A Darcy-Brinkman model of fractures in porous media*, J. Math. Anal. Appl., 452 (2017), pp. 1332–1358.
[52] M. Neuss-Radu and W. Jäger, *Effective transmission conditions for reaction-diffusion processes in domains separated by an interface*, SIAM J. Math. Anal., 39 (2007), pp. 687–720.
[53] I. Neuweiler and H. Eichel, *Restricted access effective parameter functions for the Richards equation in layered porous media*, Vadose Zone J., 5 (2006), pp. 963–977.
[54] R.H. Nochetto and C. Verdi, *Approximation of degenerate parabolic problems using numerical integration*, SIAM J. Numer. Anal., 25 (1998), pp. 784–814.
[55] F. Otto, *L1-contraction and uniqueness for quasilinear elliptic-parabolic equations*, J. Differential Equations, 131 (1996), pp. 20–38.
[56] F. Otto, *L1-contraction and uniqueness for unstationary saturated-unsaturated porous media flow*, Adv. Math. Sci. Appl., 2 (1997), pp. 537–553.
[57] I. S. Pop, J. Bogers and K. Kumar, *Analysis and upscaling of a reactive transport model in fractured porous media involving nonlinear transmission condition*, Vietnam J. Math., 45 (2016), pp. 77–102.
[58] T. Praditia, R. Helmig and H. Hajibeygi, *Multiscale formulation for coupled flow-heat equations arising from single-phase flow in fractured geothermal reservoirs*, Comput. Geosci., 22 (2018), pp. 1305–1322.
[59] F.A. Radu, I. S. Pop and P. Knabner, *Order of convergence estimates for an Euler implicit, mixed finite element discretization of Richards' equation*, SIAM J. Numer. Anal., 42 (2004), pp. 1452–1478.
[60] L.A. Richards, *Capillary conduction of liquids through porous mediums*, J. Appl. Phys., 1 (1931), pp. 318–333.
[61] N. Schwenck, B. Flemisch, R. Helmig and B.I. Wohlmuth, *Dimensionally reduced flow models in fractured porous media: crossings and boundaries*, Comput. Geosci., 19 (2015), pp. 1219–1230.
[62] B. Schweizer, *Homogenization of degenerate two-phase flow equations with oil-trapping*, SIAM J. Math. Anal., 39 (2008), pp. 1740–1763.
[63] D. Seus, K. Mitra, I.S. Pop, F.A. Radu and C. Rohde, *A linear domain decomposition method for partially saturated flow in porous media*, Comput. Methods Appl. Mech. Engrg., 333 (2018), pp. 331–355.
[64] S. Shah, O. Møyner, M. Tene, K.-A. Lie and H. Hajibeygi, *The multiscale restriction smoothed basis method for fractured porous media (F-MsRSB)*, J. Comput. Phys., 318 (2016), pp. 36–57.
[65] J. Simon, *Compact sets in the space $L^p(0,T;B)$*, Ann. Mat. Pura Appl., 146 (1986), pp. 65–96.
[66] A. Szymkiewicz, R. Helmig and I. Neuweiler, *Upscaling unsaturated flow in binary porous media with air entry pressure effects*, Water Resour. Res., 48 (2012), W04522.
[67] X. Tunc, *La modlisation des failles conductrices pour les coulements en milieux poreux*, PhD thesis, Université de Provence, 2012.
[68] J.B.W. Webber, *A bi-symmetric log transformation for wide-range data*, Meas. Sci. Technol., 24 (2012), 027001.
[69] J. Wloka, *Partial Differential Equations*, Cambridge University Press, 1987.
[70] C. Woodward and C. Dawson, *Analysis of expanded mixed finite element methods for a non-linear parabolic equation modeling flow into variably saturated porous media*, SIAM J. Numer. Anal., 37 (2000), pp. 701–724.